FINAL REPORT

High-Accuracy Multi-Sensor Geolocation Technology to Support Geophysical Data Collection at MEC Sites

SERDP Project MR-1564

JULY 2010

D.A. Grejner-Brzezinska
C. TothResearchers
The Ohio State University

SERDP
DOD ▪ EPA ▪ DOE

Report Documentation Page

Form Approved
OMB No. 0704-0188

1. REPORT DATE	2. REPORT TYPE	3. DATES COVERED
JUL 2010		**00-00-2010 to 00-00-2010**

4. TITLE AND SUBTITLE	5a. CONTRACT NUMBER
High-Accuracy Multi-Sensor Geolocation Technology to Support Geophysical Data Collection at MEC Sites	5b. GRANT NUMBER
	5c. PROGRAM ELEMENT NUMBER
6. AUTHOR(S)	5d. PROJECT NUMBER
	5e. TASK NUMBER
	5f. WORK UNIT NUMBER
7. PERFORMING ORGANIZATION NAME(S) AND ADDRESS(ES) **Ohio State University,Columbus,OH,43210**	8. PERFORMING ORGANIZATION REPORT NUMBER
9. SPONSORING/MONITORING AGENCY NAME(S) AND ADDRESS(ES)	10. SPONSOR/MONITOR'S ACRONYM(S)
	11. SPONSOR/MONITOR'S REPORT NUMBER(S)

12. DISTRIBUTION/AVAILABILITY STATEMENT
Approved for public release; distribution unlimited

13. SUPPLEMENTARY NOTES

14. ABSTRACT

15. SUBJECT TERMS

16. SECURITY CLASSIFICATION OF:			17. LIMITATION OF ABSTRACT	18. NUMBER OF PAGES	19a. NAME OF RESPONSIBLE PERSON
a. REPORT	b. ABSTRACT	c. THIS PAGE			
unclassified	**unclassified**	**unclassified**	**Same as Report (SAR)**	**47**	

1. Objective

The primary objective of the research presented in this report was to develop accurate and reliable geolocation algorithms and tools based on multi-sensor integration, to significantly improve the state-of-the-art in sensor georegistration and to support the collection of geophysical data used to characterize unexploded ordnance (UXO) and munitions and explosives-of-concern (MEC) sites in various environments. The most important tangible outcomes and achievements are: the design and prototype implementation of the new system, based on *quadruple-integration* of the Global Positioning System (GPS), Inertial Navigation System (INS), Pseudolite (PL), and Terrestrial Laser Scanning (TLS) able to address the needs for high-accuracy navigation for a non-contact mapping system in various environments. The sensor integration technology demonstrated here is innovative; while GPS/INS integration has been used to support sensor georeferencing for a number of years, integration of PLs and the laser scanning device is a novel idea.

The primary technical challenges were: (1) development of a tight integration concept for GPS/INS/PL/TLS technologies, (2) development of algorithms for ambiguity resolution for the integrated GPS/PL system, (3) testing and characterization of the stochastic properties of PL signals in order to develop optimal positioning algorithms, (4) development of methodologies and algorithms that characterize and mitigate PL signal propagation errors due to tropospheric delays and multipath disturbances, (5) development of simulation tools for the design and analysis of PL positioning geometry, (6) development of robust algorithms for TLS surface matching and integration with GPS/INS/PL technology. In particular, the project objectives were to: (1) identify and quantify performance specifications and operational requirements for UXO navigation technologies based on geophysical data requirements; (2) modify the OSU-developed GPS/INS technology and integrate it with industry standard PL and laser scanning sensors; (3) develop calibration algorithms for the proposed multi-sensor assembly; (4) perform simulations and field procedures to assess operational performance; and (5) provide the UXO community with a robust and flexible navigation technology at moderate cost, for pushcart and vehicle systems, deployable in open and wooded areas. Sensor integration is based on the Extended Kalman Filter (EKF). Navigation performance and design specifications were developed for a full suite of possible deployment scenarios. System testing of hardware and software components was conducted in both laboratory and field environments. The resulting performance was evaluated against the predefined system performance specifications to define applicability and limitations of the proposed multi-sensor technology for use in the variety of UXO mapping applications.

Although the focus for this research is the high-accuracy and automated mapping of buried UXOs, (currently in a nascent state due to the lack of a suitable high accuracy navigation system), what was developed has much wider applicability, such as underground utility mapping. At the conclusion of the phase 1 of this project the most important tangible outcome and novel achievement is: *the design and prototype demonstration of a new system, based on the "quadruple-integration" of GPS, INS, PL, and TLS that is capable of providing high-accuracy geolocation of electromagnetic sensor for a non-contact UXO mapping system.*

2. Background

Precise geolocation technology is essential for reliable detection and discrimination of unexploded ordnance in a wide range of field conditions. The detection and remediation of munitions and explosives-of-concern on ranges, munitions burning and open detonation areas, and burial pits is one of the Department of Defense (DoD) most pressing environmental problems. The MEC characterization and remediation activities using currently available technology (mostly, GPS) often yield unsatisfactory results, and are extremely expensive, due mainly to the inability of current technology to detect all MEC present at a site, and the inability to discriminate between MEC and non-hazardous items. As a result, most of the costs (90%) to remediate an MEC site are currently spent on excavating targets that pose no threat. Thus, the goal of this project is to design and implement a high-accuracy navigation device based on multi-sensor integration, that can address the stringent requirements of a man-portable geophysical mapping/imaging system in open and impeded environments, to lower the cost of remediation by improving the geolocation accuracy of MEC discrimination and thus, eliminating the excavation of non-hazardous objects.

Conducting UXO geophysical surveys using GPS-guided mapping techniques are currently the industry standard for open UXO-contaminated sites. The accuracy achievable in differential (relative) mode using GPS carrier phase observations is at the centimeter-level for short baselines (distance between base and rover is less than 5km) under strong satellite geometry and low multipath environment, and decreases with the baseline length (roughly at 1 ppm (part per million) rate). A modern approach to precise GPS positioning is the so-called network-based technique (see, for example, Vollath *et al*., 2000; Wanninger, 2002; Kashani *et al*., 2005; Grejner-Brzezinska *et al.,* 2005a), which takes advantage of the network of permanently tracking GPS receivers deployed nationwide (or locally). The network data are used to estimate the GPS errors that can be interpolated for the user's location in order to increase the accuracy of GPS position estimation. The ongoing GPS modernization is expected to further improve the positional accuracy and availability of GPS (Cabler, 2002). However, GPS is a line-of-sight (LOS) system, and requires several levels of augmentation to maintain the accuracy, continuity and reliability in confined environments. In particular, the robustness of positioning is compromised when GPS receivers are near or under trees, or in urban areas where there is partial sky view obstruction by buildings and walls. The traditional means of overcoming the gaps in navigation coverage due to satellite signal blockages is to use an inertial navigation system (INS). An INS is also the most convenient means of autonomous determination of the device/platform's position and orientation. The integration of GPS and INS can, in principle, overcome the defects of stand-alone INS (sensor errors that grow exponentially unbounded with time) and GPS (signal availability requirement) systems.

The method resulting from this research is the loose integration of PL and GPS signals together with INS and TLS measurements to deliver a precise positioning solution for geolocation of magnetic and electromagnetic geophysical sensors. Multi-sensor integration is necessary to assure accuracy, continuity and integrity of the navigation solution. It provides the first "real-world" application for this technology, and is very likely to revolutionize the existing methods for UXO detection, and drive the development of a range of products and services, many not yet even identified. The system architecture is shown in Figure 1.

The fundamental positioning concept is hierarchical, with three main levels of positioning: First, *absolute* or global positioning in open areas, which is achieved primarily using GPS/INS integration. Second, *relative medium-range* positioning under canopies or other

obstructions, where the connection between open areas with good GPS reception and areas where a GPS signal is not available can be accomplished with the PL/INS technology, i.e., PL substitutes for GPS signals for medium to long transmitter/receiver distances. Third, *relative short-range* positioning**,** where extremely high relative positioning accuracy is required, is realized by employing TLS technology that creates a surface model locally, which is used as a local reference frame. The laser scanner is connected to the GPS/INS/PL system, and thus, absolute positioning is maintained, albeit with lower accuracy, while the relative positioning accuracy in the local frame is at cm-level (see, e.g., Grejner-Brzezinska et al., 2008a-b and 2010).

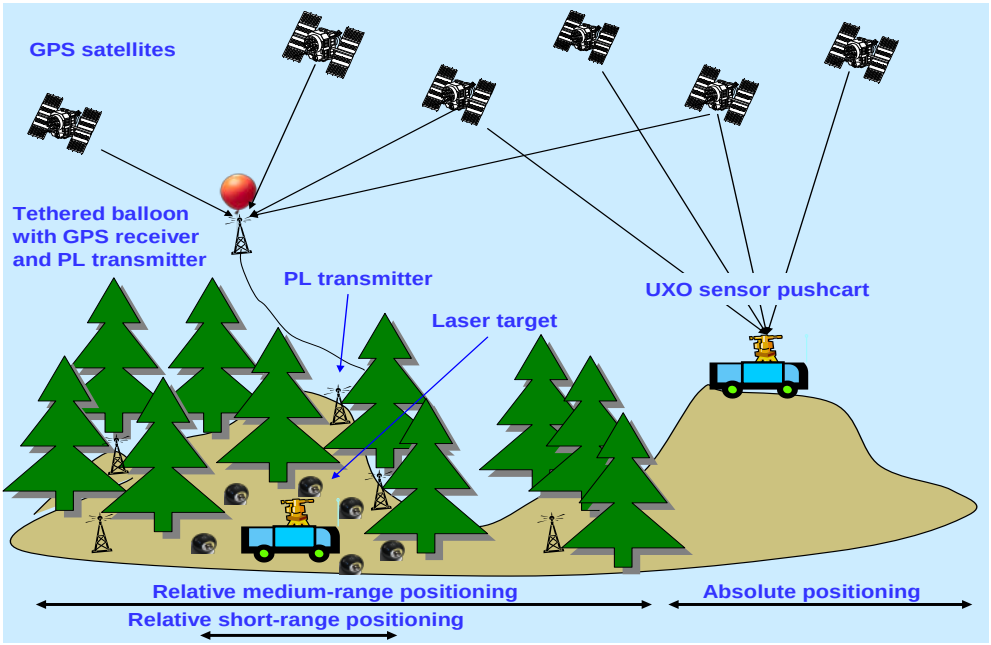

Figure 1. The concept of the MEC site survey

*The performance specifications and operational requirements***:** The selected sensors used in the demonstration prototype are the dual-frequency GPS receivers: Novatel Superstar II OEM, Trimble 5700 and Topcon Positioning System HYPER PRO. A variety of IMU sensors were studied, and sensors currently used are (1) Honeywell tactical-grade IMU 1700G, and (2) Honeywell navigation-grade, H764G. The terrestrial scanning technology is experiencing rapid developments, and the system currently used in our prototype is a Trimble GX 3D terrestrial laser-scanner, available through external collaboration with ODOT. The final recommendation for the system prototype may change as the technology evolves. The pseudolite technology selected is Locata PL available through external collaboration with UNSW.

The brief overview of TLS, with special focus on the surface matching, is presented in section 3.1. In section 3.2, an implementation overview of pseudolites for precise positioning and integration with GPS is provided. Section 3.3 presents the GPS/INS/PL/TLS integrated software (AIMS-PRO^{TM}) to incorporate the concept of a novel quadruple integration of GPS (GNSS), PL (Locata), INS, and TLS. In section 3.4, the sensor interface/data acquisition and precise time synchronization are presented. Finally, the prototype of multi-sensor UXO geolocation system is presented in section 3.5.

3. Methods

3.1 Terrestrial Laser Scanner (TLS)

A terrestrial laser scanner provides 3D surface models with sub-cm accuracy; for example, a widely used model, Cyrex 2500 scanner can provide 4 mm accuracy in the 0-50 m range for most surfaces. In our concept of multi-sensor geolocation system, this device is used to support navigation in wooded areas, where GPS may not be available, and PL network may be subject to increased multipath and partial signal blockage. High-accuracy reference surfaces, measured by TLS can be matched to cm, or even sub-cm, accuracy to detect relative motion of the platform carrying the multi-sensor assembly. The quality of the match depends on the surface geometry; for example, planar surface patches can usually be matched at accuracy better than the ranging accuracy of the laser-scanner. Using rigorous least squares 3D surface matching, complex surfaces can be matched at the level of the ranging accuracy (see, for example, Gruen and Akca, 2005). The accuracy of matching is measured in terms of the accuracy of the relative orientation parameter estimates, including position and attitude data (3+3). Thus, this technology is essential to supporting navigation in dead-reckoning mode, when GPS and/or PL signals are not accessible or limited.

The TLS is used to provide relative positions to restrict the error accumulation of INS, when the GPS and PL signals are partly or totally blocked. We designed, implemented and tested a high accuracy hybrid navigation system that can meet the stringent requirements of a man-portable geophysical mapping system, and is capable of maintaining high relative positioning accuracy in GPS-challenged environments. This navigation system is intended to integrate Differential GPS (DGPS), INS, pseudolite (PL, terrestrial RF system), and terrestrial laser scanning (TLS) and uses an Extended Kalman Filter to integrate the information from the four sensors for an optimal hybrid navigation solution.

For surface control points, the establishment of a network of spherical targets in the survey area has been proposed and tested. The spherical targets are portable, easily deployable on vertical poles or placed on the ground, and provide surface control to connect the scans performed at different platform positions. The range determined between the center of the target and TLS is used to find the coordinates of TLS by resection, and ultimately, it translates into the navigation equation. In actual surveys, if a geophysical signal is detected during the traversing of an MEC site, the high-resolution/accuracy local survey may be needed for cued interrogation. In this case 6-10 spherical targets are placed around the border of the local area of about a 10-20 m by 10-20 m.

3.1.1 Determination of the Spherical Target Coordinates

Sphere Center Determination: Research on detecting sphere center from laser point clouds is reported in (Ogundana et al., 2007), where the Hough transformation is employed to determine sphere centers and a hash table is established to solve the data storage problem. However, due to the difficulty in accurate estimation of the sphere normal with sparse points, the Hough transform method is not employed here. Instead, a four-step method for the sphere center determination has been developed, including look-up table (LUT) indexing, sphere point classification, least squares fitting, and sphere center refining.

The LUT indexing is establishing a link between laser points and a Look-up Table itself (a two-dimensional array) through horizontal and vertical scanning angles of the points. Thus, a point can be directly accessed through the memory address stored in LUT without having to

search the entire data set. The region-growing algorithm for sphere point classification segments points in a search window into different groups (objects) and then fits points of every group into a sphere. This algorithm is based on distances between a point and its eight neighbors indexed in the LUT. The measured sphere point is estimated by the Least Square Fitting method. The sphere center refining process is designed to assure that the maximum numbers of correct sphere points are included into the sphere center computation.

Sphere Center Matching: The objective of the sphere center matching is to relate the spherical targets scanned from various positions to each other. Primarily due to occlusions, the geometric configurations of the extracted sphere centers, measured at different scanning sites vary, yet normally a good number of line segments are identical. Based on this concept, the sphere center matching starts by finding one or two line segment pairs between two data sets for which the line segments have the same lengths, and thus, could link sphere centers to each other. Next, sphere center pairs between two data sets are determined based on having the same sum of distances to the end points of the matched line segments. Finally, the end points of the line segments can be matched with the same method, i.e., if an end point has the same sum of distances to the already matched points in a data set with that of an end point in another data set, they are assumed to be of the same spherical object.

TLS-Based Resection: When a minimum number of sphere centers of two scans have been matched from previous steps, the changes in position and orientation of the system platform between the two scanning locations can be derived through spatial resection (Figure 2), and subsequently used for calibrating the INS.

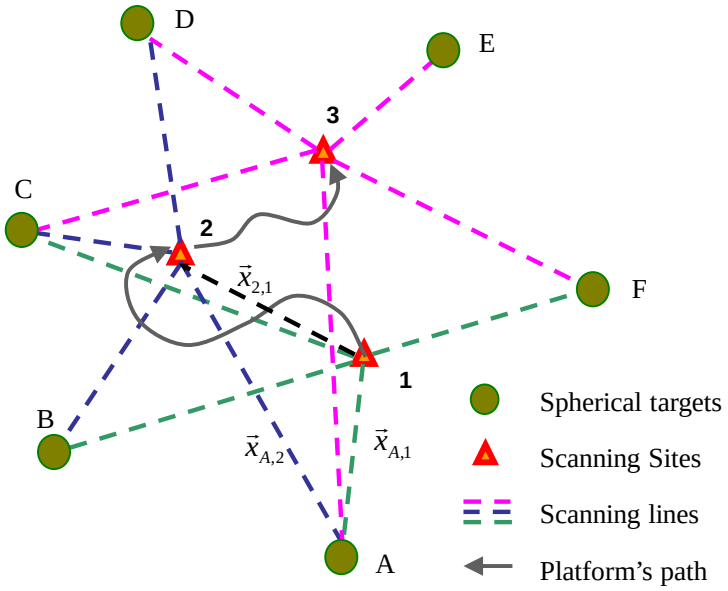

Figure 2. The spatial resection concept using TLS ranges and spherical targets.

3.1.2 Simulation Test for Surface Extraction Algorithm

An investigation of the surface extraction algorithm has been carried out, to assure fast, accurate and reliable extraction of the spherical targets, used for relative navigation with the TLS technology. The prototype processing algorithms have been implemented in the Matlab

environment. In order to study the efficiency of the point cloud registration algorithms, a set of mathematically accurate point clouds has been generated by simulating a terrestrial laser scanner, and the generated dataset was used for the verification of sphere center extraction algorithm. The simulated scenario (shown in Figure 3) was a square with an area of 4×4 m, with a 3-meter wall on one side. Two spheres with a radius of 0.20 m were set on the ground, with their center positioned at coordinates (1.0, 3.5, 0.2) and (3.0, 3.0, 0.2) in the local coordinate system. A laser scanner was mounted at coordinates (0.5, 0.5, 2.0). In this test, only the points on the walls and spheres were recorded.

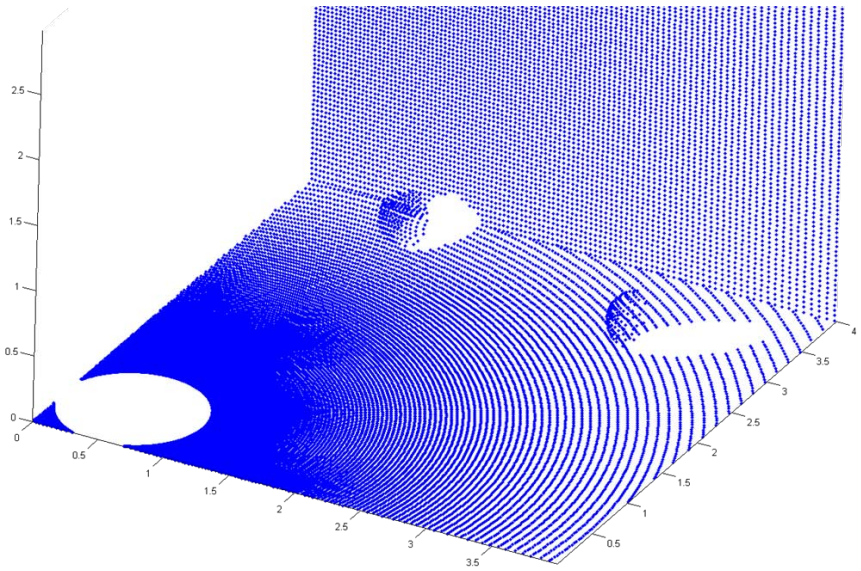

Figure 3. Simulated TLS point cloud.

After the approximate locations were determined, based on a spatial window search in the polar coordinate system, the final location of the sphere center was determined using the least squares algorithm, which included the estimation error. The extracted coordinates of the centers of both spheres are compared to the simulated reference coordinates, as shown in Table 1.

	Computed coordinates and their statistics						Reference coordinates			
	x	y	z	STD	Detected points	Iteration #	x	y	z	Total points
Sphere 1	0.997	3.499	0.190	0.004	134	6	1.0	3.5	0.2	161
	0.997	3.498	0.188	0.004	130	6				
Sphere 2	3.000	3.000	0.200	0.000	108	6	3.0	3.0	0.2	119

Table 1. The calculated center of simulated spheres and the reference coordinates.

From the above table it can be concluded that cm-level accuracy for the extracted centers of the two spheres can be achieved. Note that no observation noise was introduced to the simulated observations. The detected spherical point ratio is 80% and 90% respectively, for spheres 1 and 2, which indicates that there is still some space for improvements in the algorithm that detects points on the sphere. Investigations on that topic continue.

3.1.3 The TLS surface matching for dead reckoning mode

The performance of the target surface matching and finding the matching objects in different TLS data sets was investigated. Of the main interest is the error budget, that is, how accurately the TLS positions could be determined with respect to each other, as this sets the performance limit for the integrated GPS/INS/PL/TLS system in the dead-reckoning (DR) mode. Several surface matching methods were implemented and tested. In all tests, basketballs (used as spherical targets) randomly placed in the field were used for TLS scanning, as shown in Figure 4. The general results of these data sets showed an excellent efficiency of the range-growing algorithm, as the region-growing algorithm could match the basketballs with the success rate of 100%, despite some partial blocking by foliage and grass.

Figure 4. The field test: data collection and the deployment of spherical targets (basketballs).

Figure 5 shows the TLS point cloud of a spherical target in two views, top and side. The points on the target cover only a relatively small part of the surface, yet, the coordinates of the sphere center can be estimated with a standard deviation less than 1 cm, which has been verified by several test data sets, as reported in previous annual reports. Obviously, the number and the distribution of the points on the spherical surface have a strong influence on the sphere center coordinate accuracy as well as on the computational efficiency (i.e., the resulting number of iterations). Table 2 shows sample results from one data set.

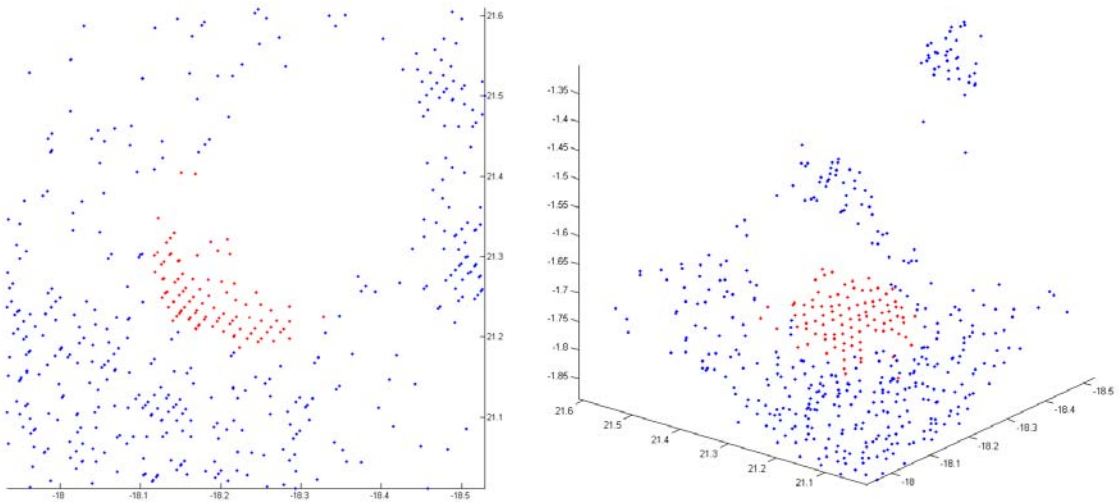

Figure 5. The extracted points of one sphere (red) and their neighboring non-sphere points (blue). Left: side view, right: top view (unit: meter).

Sphere	X (m)	Y (m)	Z (m)	Point Precision (mm)	Sphere Points	Iterations
1	17.932	-15.111	-1.972	0.6	181	2
2	21.109	-11.503	-1.832	0.7	152	3
3	19.263	-15.479	-1.851	0.5	148	3
4	14.546	-20.353	-2.009	0.7	147	3
5	19.066	-14.224	-1.869	0.8	124	3
6	16.181	-18.127	-1.916	0.8	119	3
7	24.561	-8.683	-1.759	1.0	84	3
8	22.920	-16.328	-1.709	0.9	82	3
9	25.422	-12.524	-1.657	1.0	66	3
10	21.313	-18.230	-1.790	1.5	49	3

Table 2. The estimated center coordinates of the spherical targets from the example data set.

3.2 PseudoLite (PL)

A pseudolite can be regarded as a mini-satellite that can be used for autonomous navigation and positioning in the indoor or outdoor environments using either GPS on non-GPS frequency, with cm- to dm-level accuracy. The principle of PL-based positioning systems is directly derived from the GPS technology; the system is able to triangulate the position of an object by accurately measuring the distances from the object to the array of PLs, whose location coordinates are known in a selected reference frame. It supports positioning and navigation in situations where the GPS constellation may be insufficient. PLs are usually located on building rooftops, high poles, or any high location in the vicinity of the survey area. PLs can be designed to both receive and transmit ranging signals (transceivers), and thus can be used to self-determine their own location. With some firmware modification, standard GPS receivers can be used to track PL signals.

The state of the art in PL technology is offered by Locata (see, for example, Barnes et al., 2003a and b, and 2005; Rizos et al., 2008 and 2010; Grejner-Brzezinska et al., 2010), whose approach is to deploy a network (LocataNet) of ground-based transmitters (LocataLites) that cover a chosen area with strong ranging signals of continuous coverage. These ranging signals transmit in the license-free 2.4GHz Industry Scientific and Medical (ISM) band. If a Locata receiver uses 4 or more ranging signals it can compute a high-accuracy position entirely independent of GPS. The Locata positioning technology has been designed with four key objectives: availability in all environments, high reliability, high accuracy, and cost effectiveness. Essentially, Locata allows complete control over a ground-based PL constellation, leading to an optimal positioning geometry and consistent cm-level positioning accuracy. An important feature of the Locata positioning signals is that they are time-synchronized, which allows single-point positioning similar to pseudorange-based GPS. However, unlike GPS, the sub-cm level of synchronization between LocataLites allows single-point positioning with GPS-RTK (real time kinematic) level of accuracy without the use of a reference station and data link. In addition, Locata signal strength of up to 1 Watt is much higher than the GPS signals, and thus, offers better foliage penetration within the range of a few to tens of kilometers. However, stand-alone Locata has its own shortcomings: (a) poor height accuracy (there is little variation in elevation angle between the terrestrial transmitters and receivers), and (b) no orientation information can be obtained (similar to GPS).

3.2.1 Develop integration software of Locata and GPS measurements

The Locata positioning with GPS aiding for the integration of GPS/INS/Locata data has been extensively studied. First, the offset (lever arm) between the Locata and GPS antennas must be calculated using the attitude information from the INS in real time. With this offset known, Locata ambiguities can be resolved with the GPS initial positioning result known as "Known Point Initialization" (KPI) technique. In the new generation of the Locata system this step may not be required. After the Locata ambiguities have been resolved with the KPI method, the Locata measurement (that is conceptually similar to GPS) can be fed into the Kalman filter with or without GPS data. The results from several test data sets indicated that Locata positioning could achieve centimeter level accuracy in the horizontal component, independently from GPS. Furthermore, in the integration of GPS/Locata, Locata can significantly augment the geometry of the GPS constellation. Figure 6 shows the estimated position residuals in the Kalman filter solution calibrated only by Locata's measurements. The sensitivity to the height component can be only achieved in Locata-only solution if Locata transmitters are placed on high poles or possibly on tethered balloons.

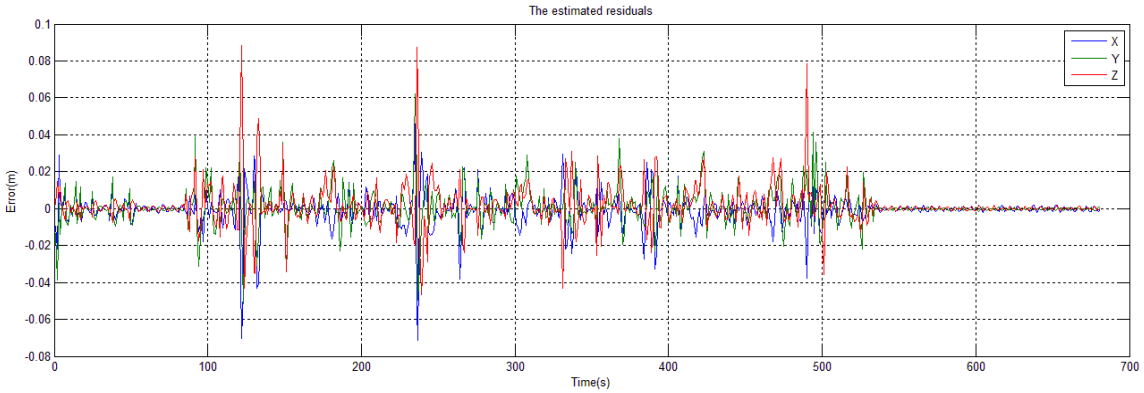

Figure 6. The estimated position errors in the Kalman filter solution for the INS/Locata integration.

In the integration of Locata/GPS, the main problem is the time synchronization between GPS and Locata data (it is an inherent feature of the Locata system that is currently, by design, not synchronized with GPS time). In addition, in kinematic applications, the alignment of the data sampling rate of GPS and Locata is also necessary and, ideally, there should be no offset between the antennas of GPS and Locata. If the data are sampled at different times and/or the antenna offset at the sampling epochs in ECEF frame is not known, the integrated positioning equations with the measurements of both GPS and Locata cannot be established. With a workaround solution, the time synchronization has been implemented externally (Locata is expected to add GPS synchronization in the future). Currently, however, the data sampling is not aligned and the antennas do not coincide in space. Therefore, the integration of GPS/INS/Locata is essential, because in this case the offset between GPS and Locata is obtained based on the attitude information from INS, as already explained; subsequently, Locata measurement can be passed to the Kalman filter independently as measurement update. The software implementation of GPS and Locata measurement integration was finished and tested based on the field data.

The Locata ambiguity resolution is an important component of Locata positioning. In the integration of GPS/INS/Locata, as mentioned above, the ambiguity was solved successfully with the KPI method. However, in the Locata standalone positioning mode, there is still work

required to resolve integer ambiguities; this is related to the current limitations of the Locata hardware, as already explained above. In the synchronized mode, however, the clock errors are the same for all LocataLites (time-synchronized transmitters); thus, these errors can be completely removed with the clock error of the Locata (receiver) using the single difference model between LocataLites. Furthermore, in this case, if the initial phases of LocataLites signals on both frequencies were aligned, the wide-lane combined ambiguity would be an integer, and thus, could be solved relatively easily, as the wavelength of the wide-lane measurement is very long (up to about 6 meters). However, this is not an algorithmic issue that can be addressed by this research team; the solution requires changes in the hardware design of the Locata system, so it is an entirely manufacturer-dependent matter.

Based on the float-ambiguity bridging method proposed in this research, the cycle slip issue has been successfully addressed in the Locata system. Based on several tests, it was confirmed that this method could detect cycle slips with a success rate of almost 100% if there were five or more GPS satellites or LocataLites, despite the fact that the wavelength of the carrier frequency of Locata is only about 10 centimeters.

In *Locata's* current system design, the floating point carrier phase ambiguities are commonly solved through static initialization on a precisely surveyed point known as KPI, as already explained. However, in practical kinematic applications it would be convenient to be able to resolve the ambiguities "on-the-fly". The researchers from the University of New South Wales (UNSW), the collaborative partner of this project, and close collaborators of Locata Inc., developed an on-the-fly ambiguity resolution algorithm based on the concept of nonlinear batch least squares estimation, which proved to be suitable for calculating an ambiguity float solution. This method has been made available to the OSU research team.

3.2.2 Characterization of the stochastic properties of Locata signals

Based on the entirely ground-based constellation of the Locate transmitters, Locata system has much different characteristics for tropospheric delay, multipath and signal fading, as compared to GPS. For example, in the currently used point positioning mode in the Locata system, the tropospheric delay cannot be removed or mitigated by the observation from the reference station. Also the model for GPS tropospheric delay is quite different, as GPS signals travel through the entire tropospheric layer, while Locata signals are transmitted near the ground. Our tests indicated that if the influence of the tropospheric delay is ignored in the Locata positioning, the coordinates could drift up to about 20 centimeters in 10 minutes, even in a small area where the atmospheric conditions remain comparable. Thus, this error is time and space dependent. To resolve this problem, an appropriate tropospheric delay model for Locata was established in cooperation with UNSW. In the subsequent tests, the model showed a satisfactory performance, as there was no obvious coordinate drift.

Concerning the deployment requirements of the system, the multipath of the Locata signal should be considered more carefully, because the operating environment of the target application is expected to be extremely difficult. As compared to other error sources, modeling and prediction of multipath is particularly complex. In the GPS practice, the concept of multipath is rather well understood (but not fully resolved or mitigated), as a signal transmitted from a satellite can follow a multiple number of propagation paths to the receiving antenna. This is due to the fact that the signal can be reflected to the antenna off the surrounding objects, including man-made objects and the earth's surface. Techniques to reduce multipath error have been a focus of considerable research for many years. In GPS environment, the most common multipath reflector is the surface of the earth itself, and this

fact is usually exploited by manufacturers through the antenna design and elevation cut-off angles in data collection and processing. However, for Locata, a ground-based RF system, the signal from the transmitter typically arrives at the receiver antenna at a very low (less than 10 degree) or negative elevation angle. As a result, these signals are subject to a severe form of multipath known as multipath signal fading. The signal fading manifests itself as severe signal power fluctuations. These are due to constructive and destructive multipath resulting from low incident signal transmits angles that cause reflections off the surface of the earth. This phenomenon has received considerable research in RF communications, but not in RF-based terrestrial positioning.

Figure 7. The installation of the LocataLite antennas in the test at OSU campus.

Our tests showed strong multipath signal fading effects; the received signal power varied significantly at the receiver antenna due to destructive and constructive multipath. Constructive multipath causes the received signal power at the receiver antenna to be greater than expected, whilst destructive multipath causes the signal to be weaker than expected. To mitigate this problem for the Locata system, the spatial diversity technology is deployed to deal with the multipath issue. In this method, there are two transmitting antennas and one receiving antenna for every LocataLite, as shown in Figure 7, which allows two signals with different PRN codes at the same frequency (in the 2.4GHz band) to be transmitted. Thus, physically separating the two transmitting antennas has been results in signal spatial diversity. Our initial tests confirmed a good performance of the spatial diversity technique, especially for carrier phase observations.

The tropospheric delay and multipath errors and their modeling/mitigation are complex issues for Locata-based positioning, and they need additional research, including a number of test data sets, to arrive at some empirical conclusions. The tropospheric delay parameters are adaptively adjusted to weigh the measurements from the two spatially separated antennas to optimize the performance. Since OSU does not own a Locata system, we rely on our partners', UNSW and AFIT, support to provide field data and some error modeling aspects. This is still an ongoing activity that may continue in Phase II of the project.

In Locata Tropospheric Correction (LTC), the tropospheric correction is employed to the difference between the distance of LocataLite and rover position and the distance of LocataLite and a known point. By taking the difference between the two distances the LTC not only takes care of the distances that are not included in the ambiguity resolution but also uses the benefit of KPI, which includes its ability to absorb the effect of radio interference and biases. A comparison between LTC and other pseudolite based tropospheric models such as RTCA (Radio Technical Commission for Aeronautics) and Modified RTCA is depicted in Figures 8-10 for positioning at an unknown point. These figures show that using the LTC, high accuracy is possible without impacting VDOP (vertical dilution of precision) and HDOP (horizontal dilution of precision). In terms of accuracy, the LTC performs better than the other models used in the early PL software implementations.

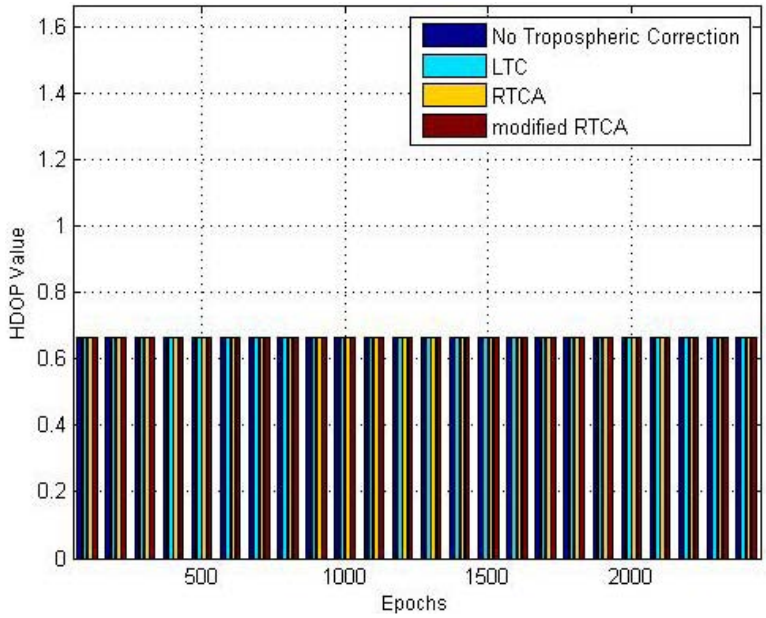

Figure 8. HDOP comparison between different tropospheric models for positing at an unknown point (Politi et al., 2009).

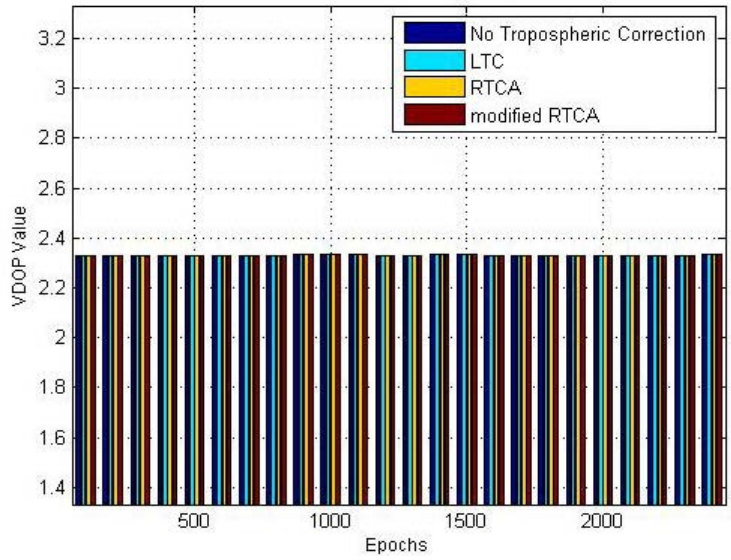

Figure 9. VDOP comparison between different tropospheric models for positing at an unknown point (Politi et al., 2009).

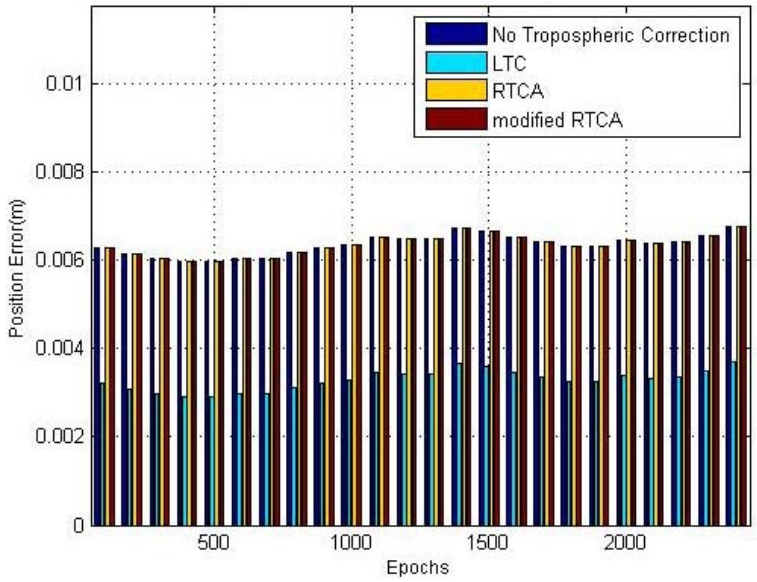

Figure 10. Accuracy comparison between different tropospheric models for positing at an unknown point (Politi et al., 2009).

3.2.3 The PL and spherical geometry

In the independent Locata positioning, the geometry is the very important issue, because the LocataLites are typically placed on the ground. After the initial study, it was confirmed that if the LocataLites are set on a level plane, the vertical component of the coordinates is correlated with the clock error of the Locata system (receiver). In fact, the system will have no solution if the LocataLites are set at a same elevation and all distances to the Locata receiver are the same, as in this case the height is completely correlated with the clock error. In the configuration shown in Figure 11, if the LocataLite at point D is moved to point D', the system will fail. Note that the poor solution in vertical component has very limited influence on the horizontal coordinates. However, if the plane, on which the LocataLites are set, is

tilted, the correlation between the coordinates and the clock error will project to the horizontal components. Therefore, in practical applications, it is necessary to avoid installing all the LocataLites in a plane, whether it is leveled or tilted. Obviously, it is necessary to have at least four LocataLites for 3D positioning, and the number of LocataLites has significant contribution to the final performance, especially in the vertical component.

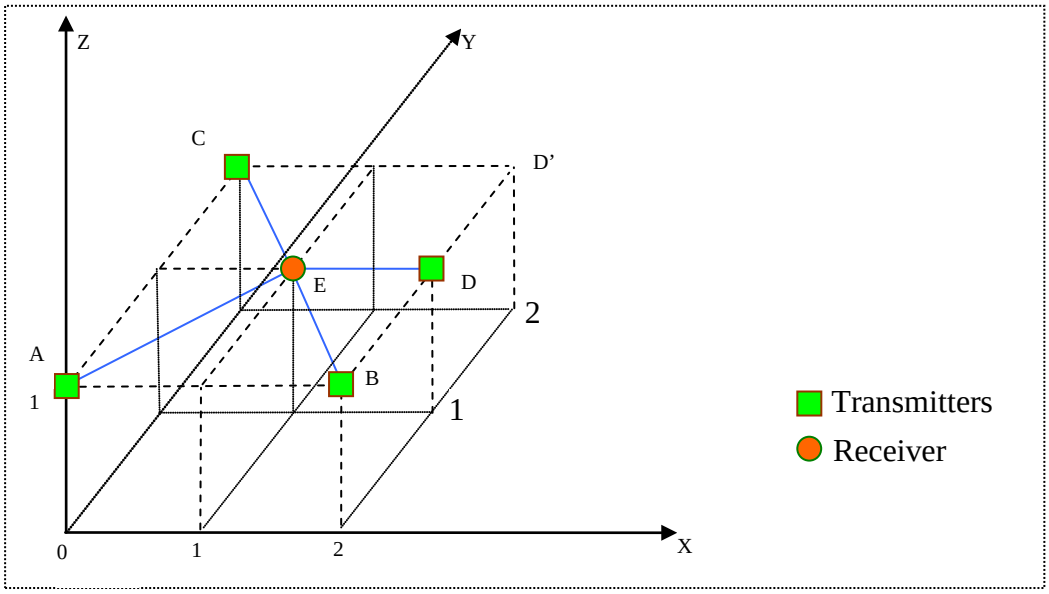

Figure 11. The deployment of the LocataLites (transmitters and receiver) in the prototype system.

The quality of the estimated ambiguity float solution of the Locata depends on several factors, the most critical being the geometric characteristics of the transmitter network. In some typical network setups, where all transmitters are placed at a similar height, the poor observability of the height component can prevent the on-the-fly ambiguity resolution from achieving the desired centimeter-level positioning accuracy. The UNSW test network consisting of only four LocataLites (Locata transceiver, marked red in Figure 12) suffers from this geometry deficit. Adding further LocataLites near the ground level (marked blue in Figure 12) significantly improves network geometry and ensures centimeter-level positioning accuracy (Figure 13) with float ambiguities solved on-the-fly.

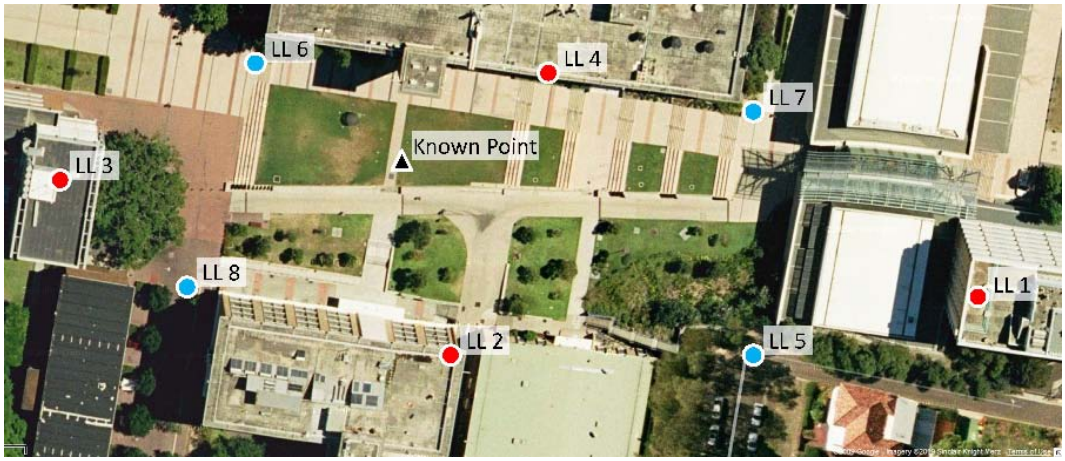

Figure 12. LocataLites distribution on the UNSW campus (Politi et al., 2009).

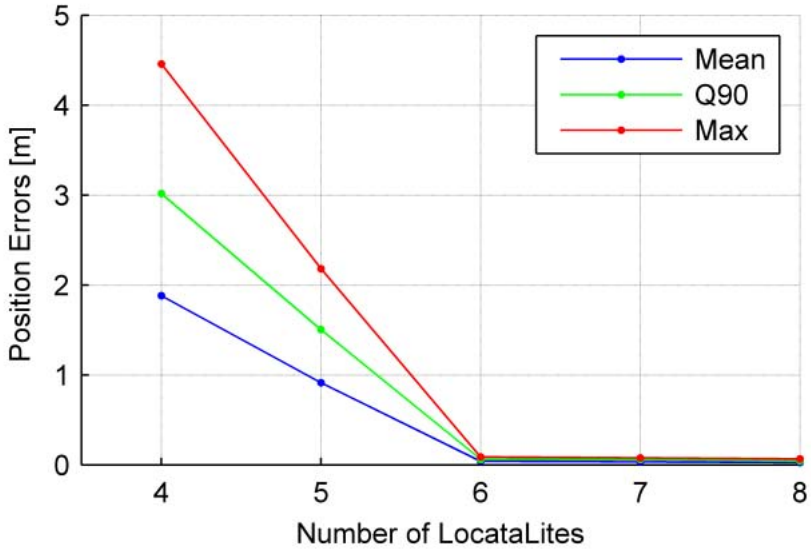

Figure 13. Positioning accuracy with Locata vs. LocataLites network design (Politi et al., 2009).

The ongoing development by the Locata manufacturer will ensure that the ambiguities will be integers, which will allow the application of integer ambiguity estimation concepts well known from GPS. In anticipation of the system's future design, measurement data with integer ambiguity terms was simulated, and the integer ambiguities were successfully determined from the float solution using the LAMBDA (least-squares ambiguity decorrelation) method. The simulation results indicate that for the selected network setup and receiver trajectory, centimeter level coordinate accuracy with on-the-fly ambiguity resolution for Locata is possible (Politi et al., 2009).

The method of using the Dilution of Precision (DOP) factor for the analysis of target distribution provides some insights to the operational conditions for TLS-based navigation. Similar to PL/GPS positioning, the geometric distribution of the spherical targets relative to the laser scanner will affect the positioning accuracy of the laser scanner and thus the navigation accuracy of the integrated system. By comparing the DOP values for different relative distributions of spherical targets and laser scanner (TLS), useful information can be obtained regarding the desired target distribution; in addition, performance metrics can be derived.

In order to study the effects of geometric distribution, different combinations of relative geometry between the scanner and the targets were tested. As shown in Figure 14, for different selections of 4 targets from the sequentially numbered 10 targets surrounded the scanner, target case study 1, which includes targets 1, 3, 6, and 9 that are almost evenly distributed within the 10-target constellation, has the minimum HDOP, VDOP, and PDOP values of 1.03, 2.23, and 2.45, respectively. For the other three 4-target cases 2-4 that include other targets (2, 3, 4, 5; 4, 5, 6, 7; and 7, 8, 9, 10 respectively), the DOP values are 2-3 times higher than the evenly distributed case. For the detail of other simulation scenarios, such as effects of the relative position between spherical targets and the scanner, effects of increasing target elevation, and effects of different numbers of targets used, we refer to (Wang et al., 2010).

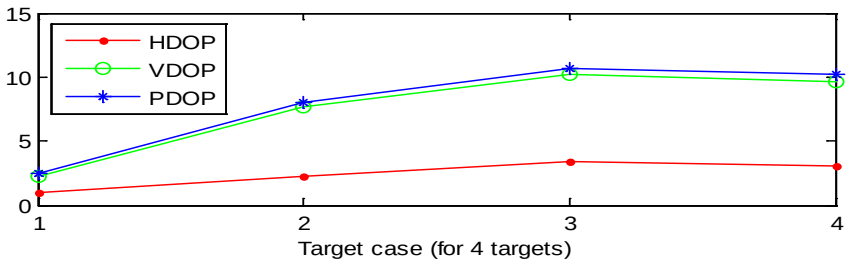

Figure 14. DOP values for different selections of 4 targets from the original 10-target constellation (case 1) for TLS position 1.

The simulation results indicated that the optimum distribution of the spherical targets is achieved by an even distribution on the ground around the center of the area of interest. For the case of a TLS surrounded by ten targets located about 8 meters horizontally from TLS, the PDOP values can be as low as 1.36. As long as the scanner is surrounded by the targets, the DOP values are very comparable, and there is no need to elevate any targets, as it does not result in a significant decrease of the DOP values (note locating targets on some bolsters would significantly increase the workload in case of no terrain undulation). If, due to operational constraints in the field, the optimum distribution cannot be attained, the target cluster should be as close as possible to the center of the area of interest. In this case, some targets can be put on poles to decrease the DOP values. Another requirement of target distribution is that targets should be placed at locations that will assure that a significant number of targets can be observed from different scanning sites. The worst case, when only a few targets clustered outside of the scanner can be observed, should be avoided.

3.3 GPS/INS/PL/TLS integration software

The GPS/INS software, developed earlier at OSU, called Airborne Integrated Mapping System (AIMS), has been utilized for this project. The AIMS is based on the tight integration approach, where the EKF optimally estimates position, velocity, and attitude errors, as well as errors in the inertial and GPS measurements. Tight integration supports cycle-slip fixing in the GPS data and allows robust OTF (on-the-fly) ambiguity resolution. Implementation of closed-loop INS error calibration allows continuous, OTF error update that bounds INS errors, leading to increased estimation accuracy. In AIMS, the inertial strapdown algorithm is implemented for processing the raw IMU data, providing the navigation solution. The attitude determination algorithm uses quaternions, whose numerical stability is superior to the direct cosine method. A single EKF, with number of states equal to 21 plus the number of GPS double differences, is then used to process the GPS double-differenced phases, combined with the inertial solution. The state unknowns, as mentioned above, are errors in position, velocity, and orientation, three biases and three scale factors for the accelerometers, three gyro drifts, two deflections of the vertical and the gravity anomaly. In addition, GPS ionospheric delay is estimated for every satellite in the solution (Table 3). Also, GPS-INS lever arm errors can be optionally included in the state vector. These are related to the unknown offsets of the GPS antenna from the IMU center. Figure 15 illustrates the basic modules of the GPS/INS integrated system design, indicating possible various GPS solution types that can support mainly loose integration approach, while Figure 16 shows the initial AIMS-PRO^{TM} design and workflow (more details are provided in the following sections).

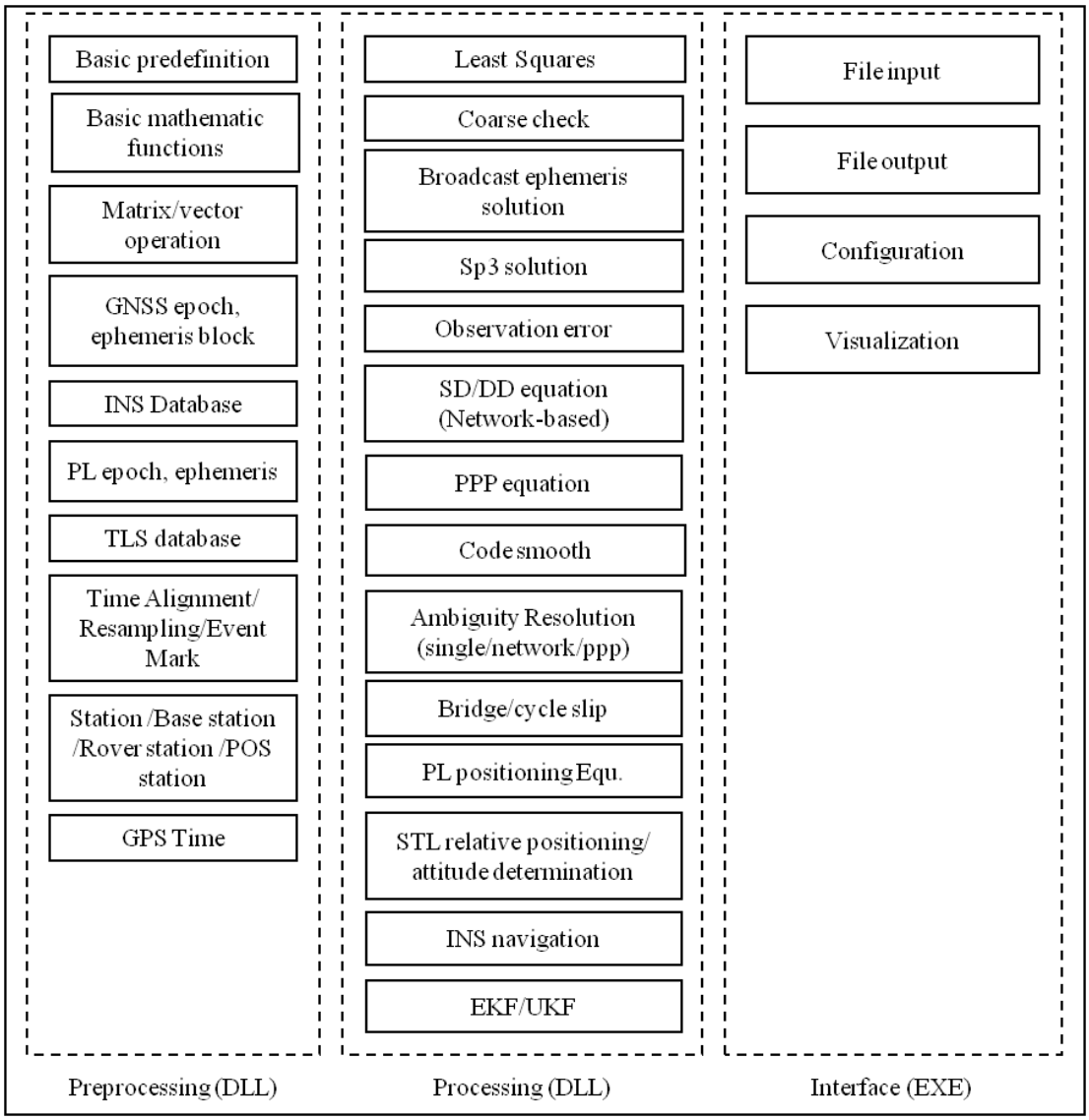

Figure 15. The basic module of GPS/INS integrated system software.

Kalman Filter States		States #
Navigation Parameters	Position errors Velocity errors Attitude errors Heading errors	3 3 2 1
Accelerometer Errors	Biases Scale factor errors	3 3
Gyro Errors	Drifts	3
Gravity	Deflection Anomaly	2 1
GPS Errors	Ionospheric delay Double-difference white noise	Number of DD 1 cm

Table 3. AIMS system parameters.

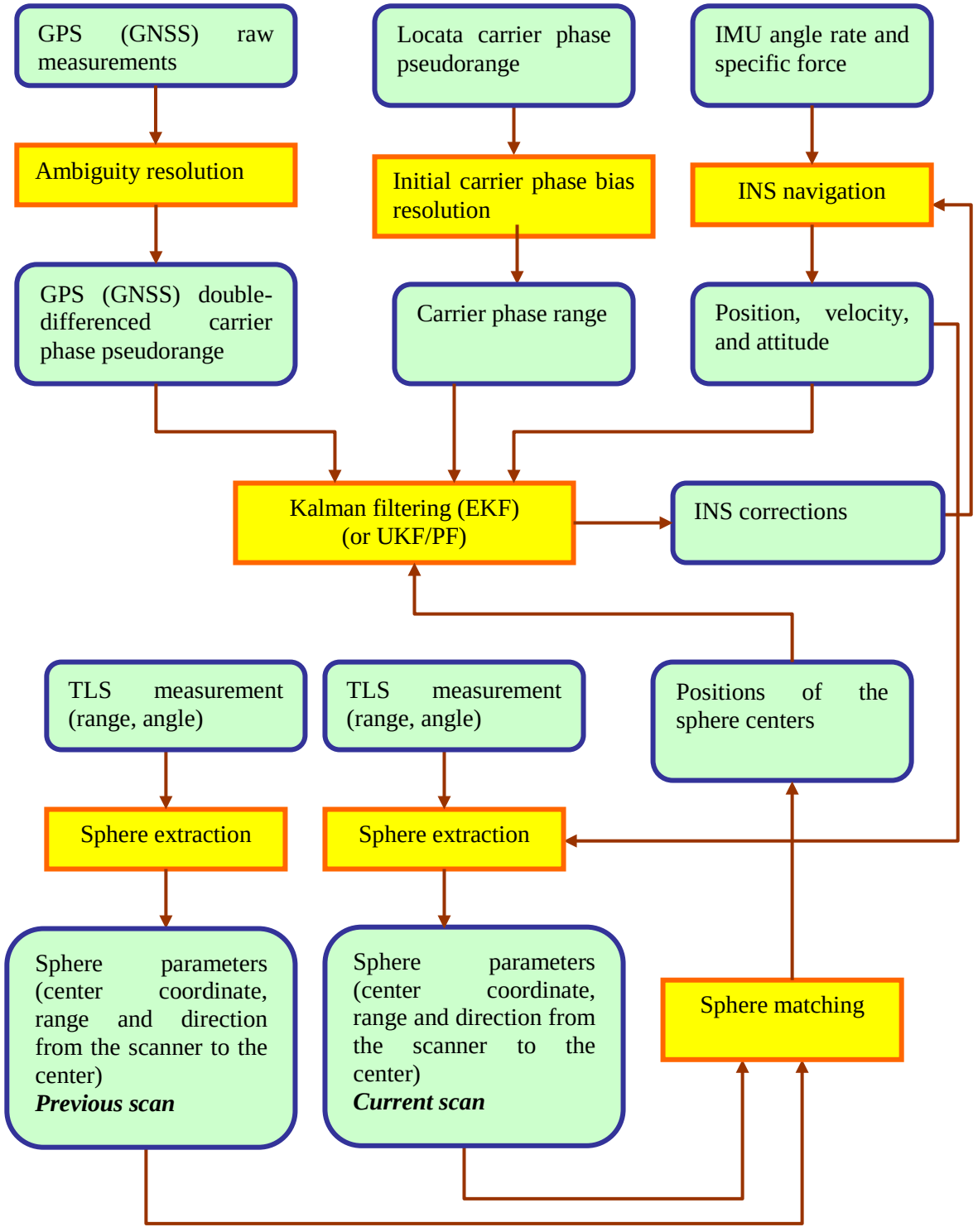

Figure 16. The workflow of the integrated DGPS/PL/INS/TLS system; DGPS stands for differential GPS.

3.3.1 AIMS-PRO™

The original OSU GPS/INS integrated system, AIMS™, was completely redesigned and extended to incorporate the concept of a novel quadruple integration of GPS (GNSS), PL (Locata), inertial technologies (INS), and TLS; the old AIMS™ was based on a single tight GPS/INS integration module. The new software, named as AIMS-PRO™, has the following major system and software design characteristics:

- Multiple approaches to GPS solution (in loose integration mode):
    - Single baseline differential kinematic solution
    - Network-based differential kinematic solution
    - Precise point positioning technique (PPP)
- Handles various IMUs classes from navigation- through tactical to consumer-grade sensors
- Loose and tight integration modes (tight mode illustrated in Figure 20)
- Accepts feedback from the imaging module to implement terrain-referenced navigation in GPS-challenged environments:
    - TLS with specialized targets for highest navigation accuracy
- For users' convenience, the computations are performed in various coordinate frames of choice, including local frames and ECEF
- Multiple operating modes for the coupling procedure, including one-direction and three-direction processing (i.e., three-direction=forward processing used for calibration/alignment followed by backward processing and smoothing)
- Improved reliability due to increased redundancy (quadruple integration of signals)
- Flexible design structure, based on the component software technology
- Improved error diagnostics capabilities

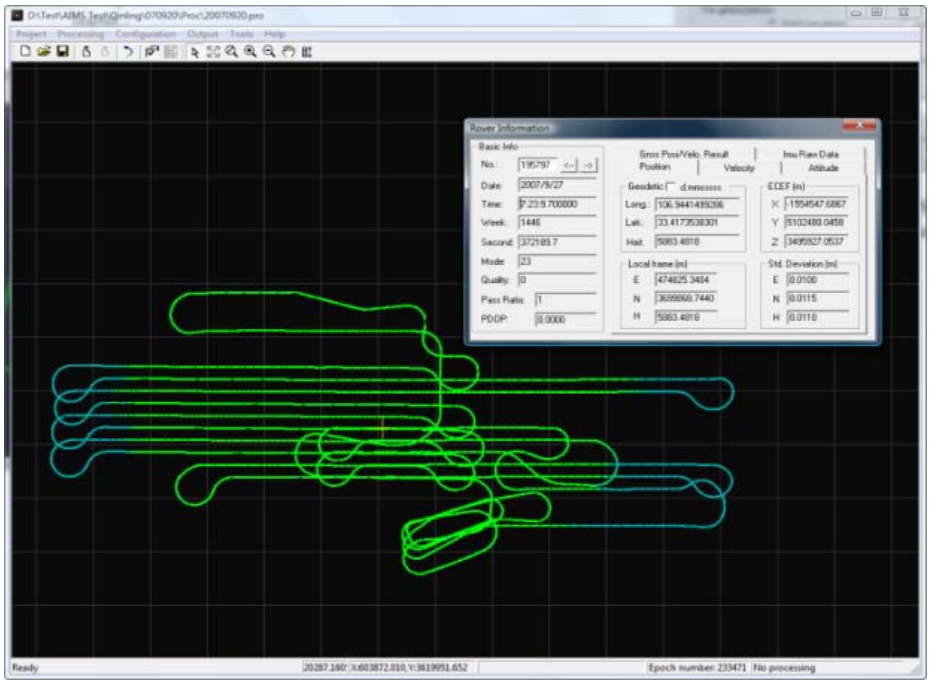

Figure 17. AIMS-PRO™: main user interface.

Figures 17-20 illustrate various interface components of the AIMS-PRO™ design. The main interface, shown in Figure 17 provides access to all raw and processed data and other information, including time, raw sensory data, position, velocity and attitude, etc. The input interface is designed for handling all major types of input data, including initial location and orientation parameters, see Figure 18. The data processing dialogue, shown in Figure 19, provides a flexible interface to all configuration and control parameters defining the data processing modes. For example, the initial parameter settings for EKF allow for the selection of the sensor models suitable for a particular class of sensors or a specific IMU. GNSS processing parameters, error tolerances, ambiguity resolution parameters, etc. are also defined

through this interface. Figure 20 shows the data flow in the AIMS-PRO™ system for the tight coupling of the GPS/INS/PL/TLS integrated system. For more details, see, for example (Grejner-Brzezinska et al., 2008a-b and 2010).

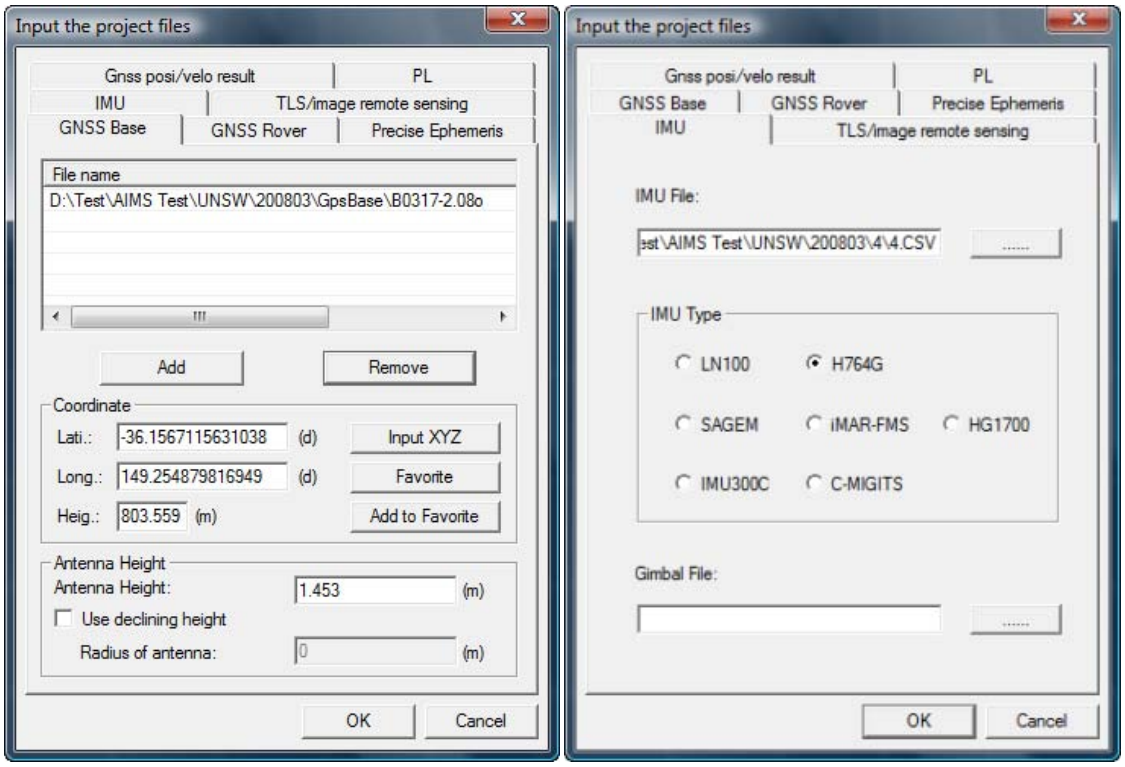

Figure 18. AIMS-PRO™ interface: GPS and IMU data input dialog boxes.

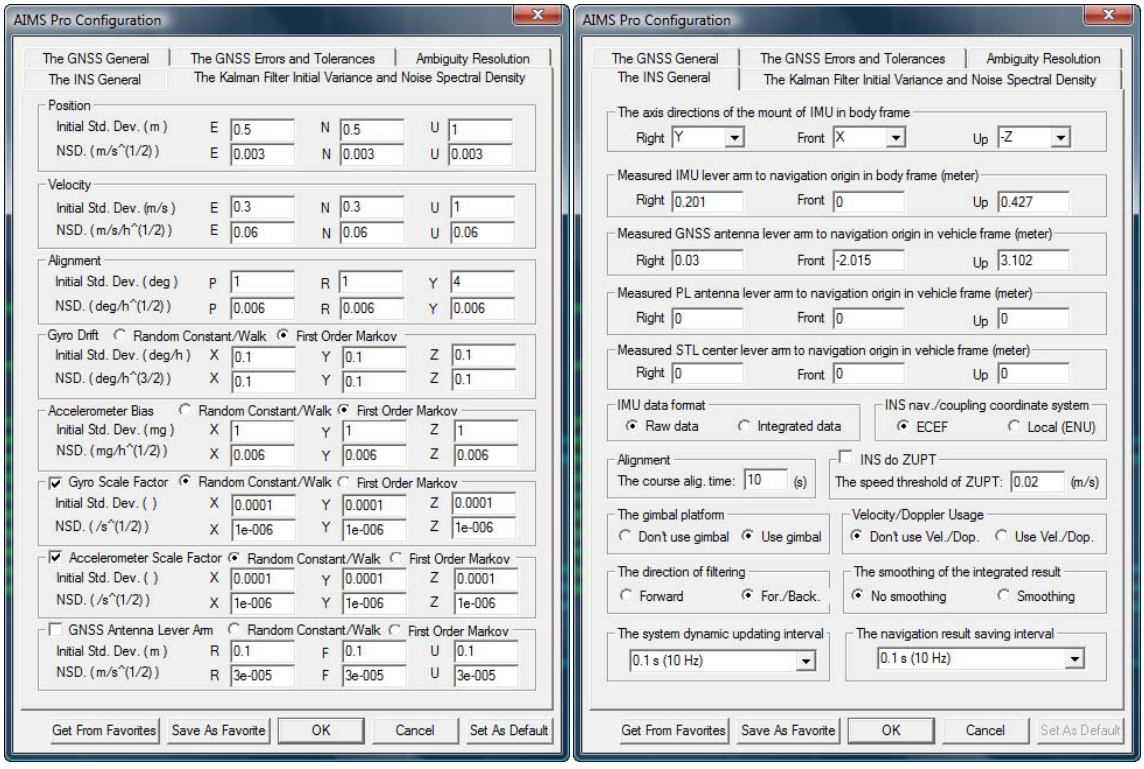

Figure 19. Snapshot of AIMS-PRO™ interface: configuration and control parameters.

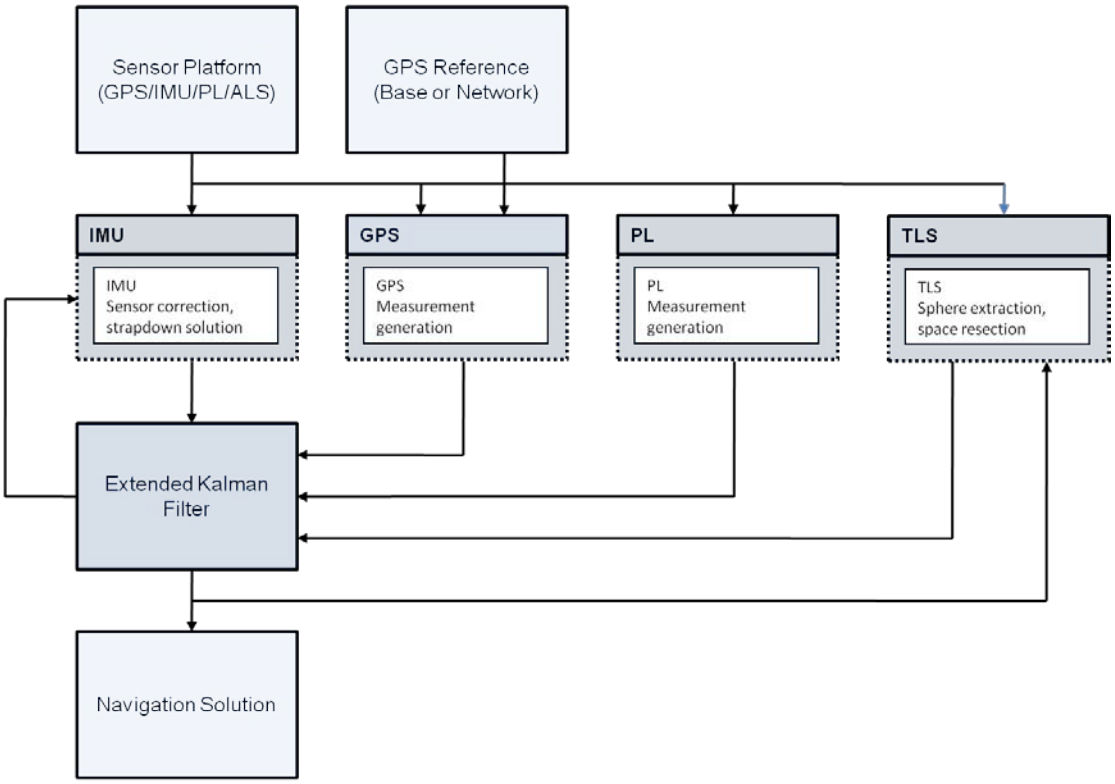

Figure 20. AIMS-PRO™ design architecture for the tight coupling mode.

Various tests with real data verified that the target performance of the integrated system could be reached. The absolute positioning accuracy was achieved at centimeter-level (i.e., the DGPS short-baseline accuracy in horizontal coordinates) in open and moderately blocked environments, and the relative accuracy was maintained at about 1 cm level in heavily obstructed environments with the TLS-supported navigation. Figures 21-24 illustrate the examples of the performance evaluation results of the system for the 2008 Numeralla, Australia field tests.

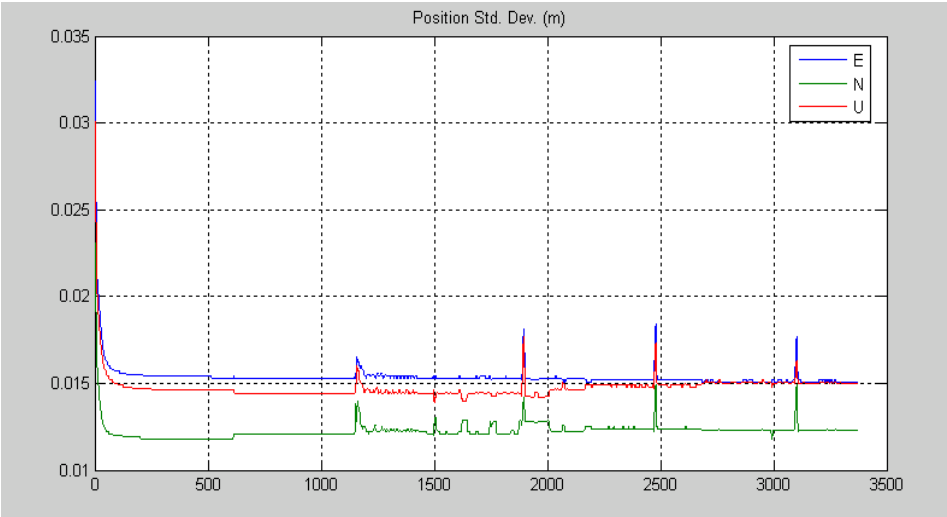

Figure 21. The standard deviation of the position in the integrated GPS/INS/Locata solution.

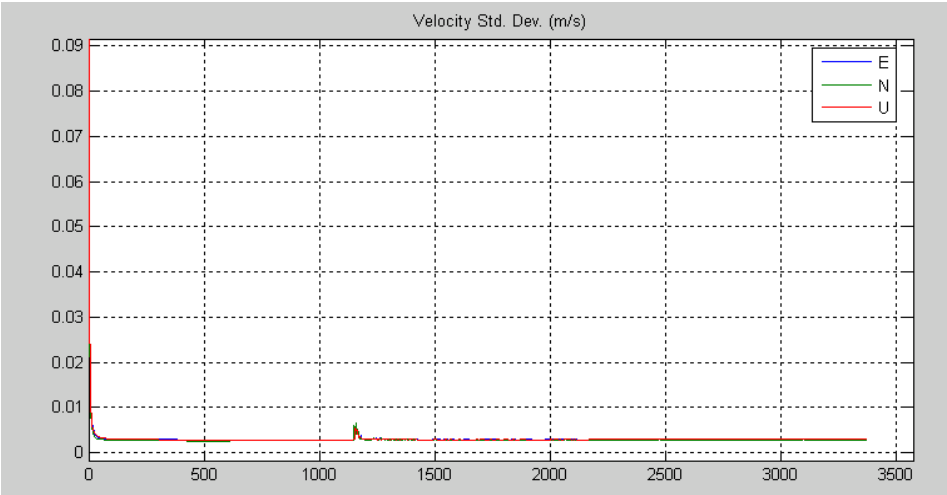

Figure 22. The standard deviation of the velocity in the integrated GPS/INS/Locata solution.

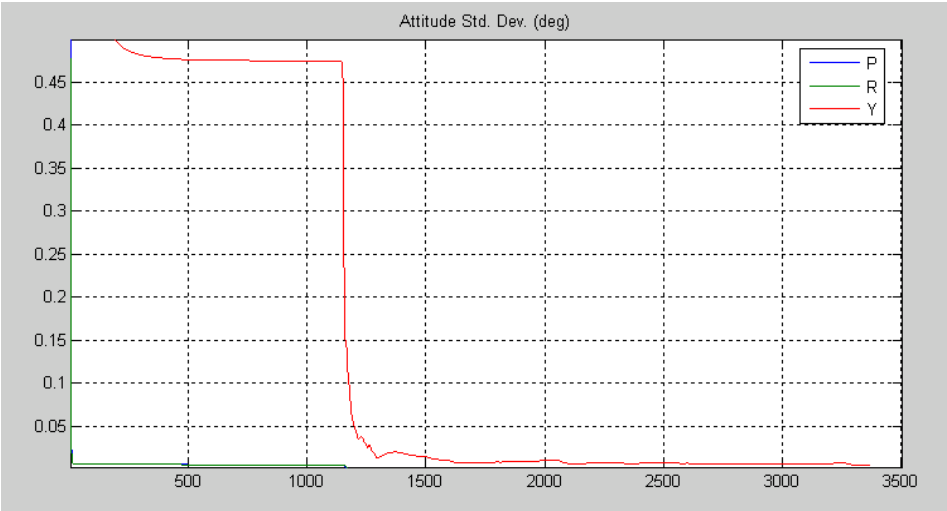

Figure 23. The standard deviation of the attitude in the integrated GPS/INS/Locata solution.

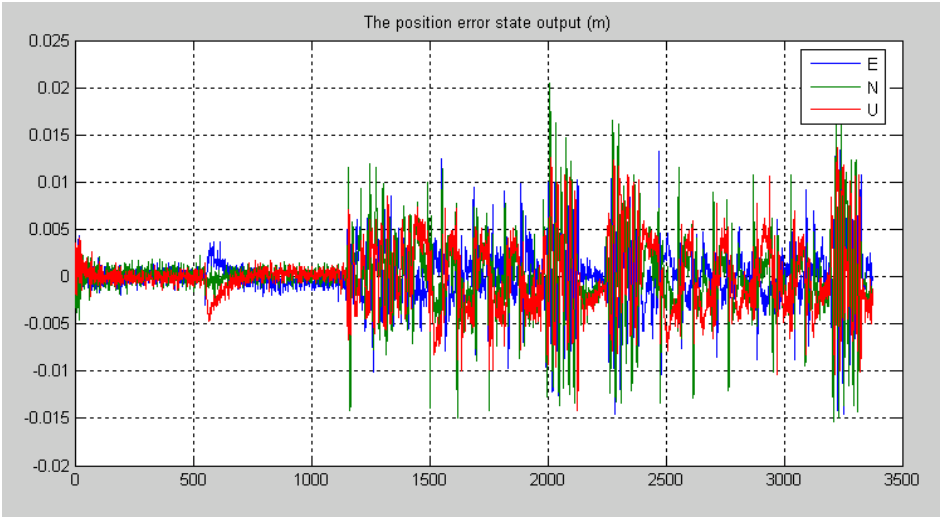

Figure 24. The sub-state of position error in the Kalman Filter.

3.3.2 The refining of IMU stochastic model and the implementation of the GPS/INS integration

The stochastic characteristics of IMUs of different grades could vary over a large range; furthermore, there could be sometimes considerable variations in the stochastic parameters for the same grade IMUs from different manufacturers, or even for the same IMU at different time or in different environments. This issue is still a subject of research. In AIMS-PRO^{TM}, a significant attention was paid to incorporating several types of IMU stochastic models for different IMU grades and brands. The tests showed that the use of suitable IMU stochastic model with adequate parameterization is essential to achieving the highest accuracy of the integrated system.

Figures 25-26 show the gyroscope outputs from the EKF with different stochastic models. Although the figures look very similar, the solution based on the first-order Markov process model is slightly better and, in many cases, could improve the standard deviation of position, for example, from 3 to 2 cm.

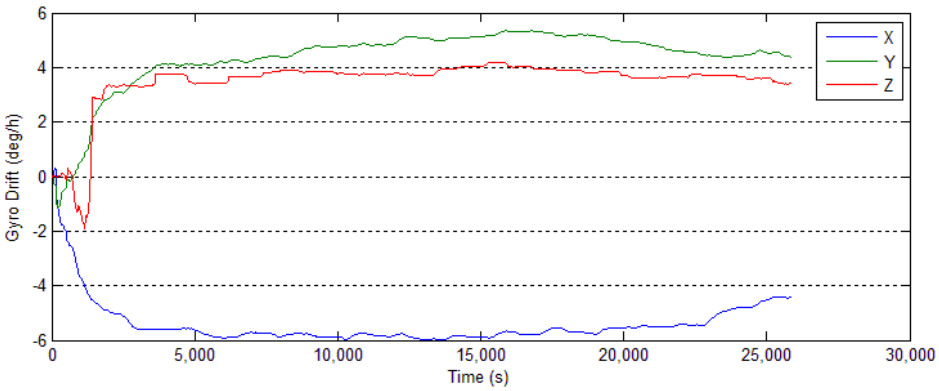

Figure 25. The estimated gyro drifts using random walk model.

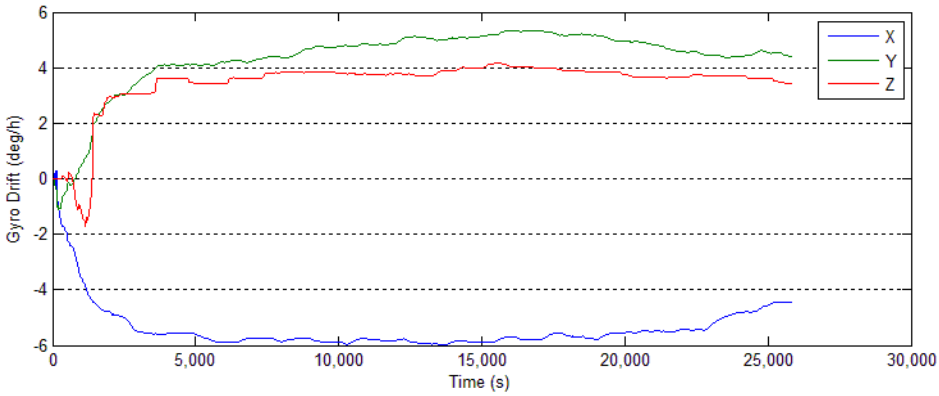

Figure 26. The estimated gyro drifts using first-order Markov process model.

Furthermore, statistical test was performed to find out the suitable parameters of stochastic model (see Li *et al.*, 2010). Customized parameters from Allan Variance analysis (see Figure 27 and Figure 28 for examples of Allan Variance) and heuristic EKF tuning method, plus manufacturer's specification were respectively used in the tests. GPS outages of 10 seconds, 60 seconds and 300 seconds were simulated to judge the performance of each parameter set. Table 10 shows the statistical results for each gap duration. It can be noticed that for GPS outage of 10 seconds and 60 seconds, all three parameter sets delivered a comparable

performance. However, when the GPS gap duration reaches 300 seconds, the heuristic method provided a much better solution than the Allan Variance-based parameters and the manufacturer's specifications, with the total position error of 33 m, as compared to ~64 m for the other two results.

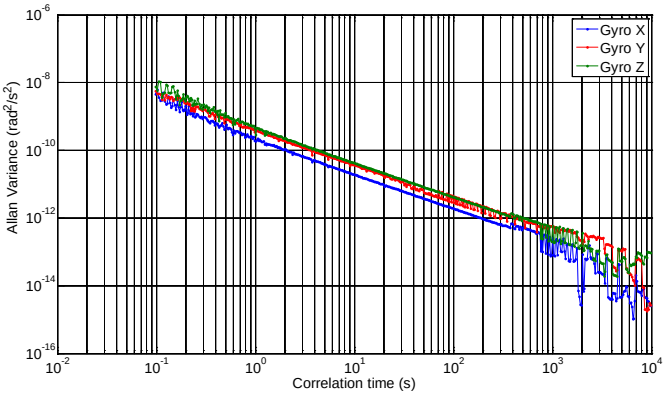

Figure 27. Allan Variance of H764G gyroscopes.

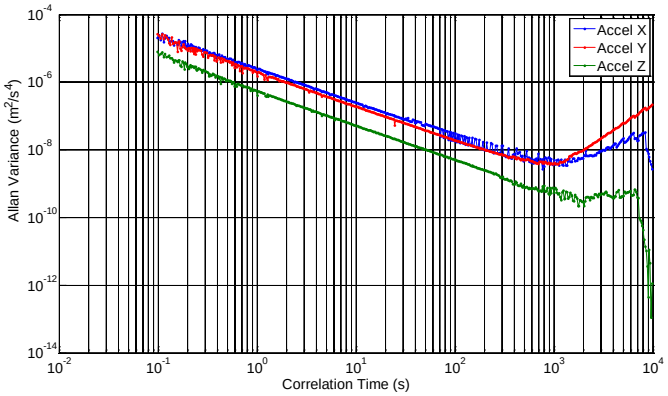

Figure 28. Allan Variance of H764G accelerometers.

GPS Outage	Allan Variance		Manufacturer's Specification		Heuristic Method of EKF Tuning	
	Average Error (m)	STD (m)	Average Error (m)	STD (m)	Average Error (m)	STD (m)
10s	0.330	0.208	0.355	0.190	0.393	0.155
60s	3.891	1.128	3.759	1.256	2.962	1.894
300s	63.992	24.739	63.714	30.410	33.133	13.897

Table 4. Average navigation errors for different GPS outage duration and different stochastic error characteristics.

The implementations of different approaches to GPS/INS coupling for post-processing applications were tested. In the post-processing mode of the Kalman filter, the smoothing is an effective technique to improve the final position accuracy of the system. In this project, a different three-way filtering-based smoothing was proposed, which is based on triple filtering, namely first forward, backward, and second forward; note the first forward filtering

is just considered as an IMU initial calibration and is eventually discarded. The results of the backward and the second forward filtering are smoothed for the final output of the system. This way, the system can use the whole forward filtering for the IMU initial calibration, so the usual maneuvering of the navigation sensors after the starting up period is not necessary. Figure 29 shows the convergence of the gyroscope drifts in a several-hour test, which indicates that data of about one hour would normally have to be discarded from the solution under normal (one-way) processing. However, in the three-way filtering solution, this section can be recovered with the accuracy comparable to the rest of the trajectory. Figures 30-31 show the comparison of the final output of the three-way and one-way filtering methods. The results in the figures clearly show that the heading accuracy of the weakest area improved from 0.02 deg to 0.008 deg.

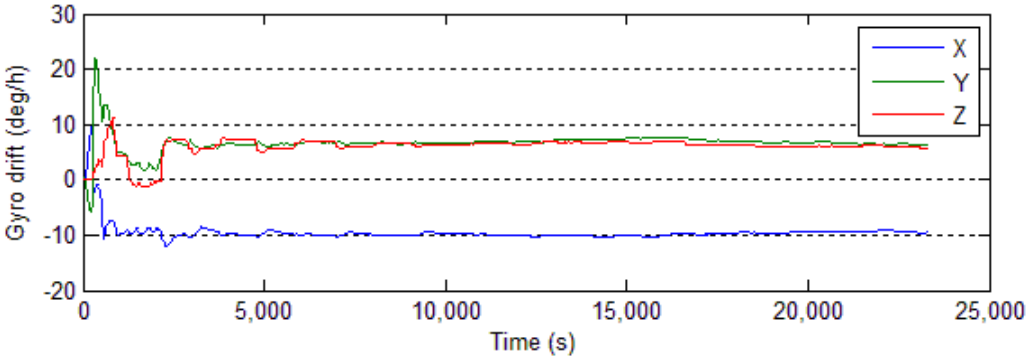

Figure 29. The convergence of the gyroscope drifts in the first forward filtering.

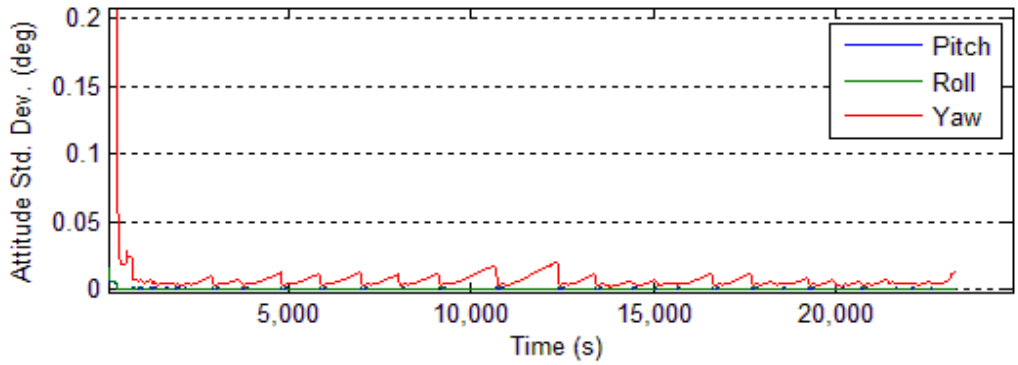

Figure 30. The STD of the attitude angles in the forward filtering.

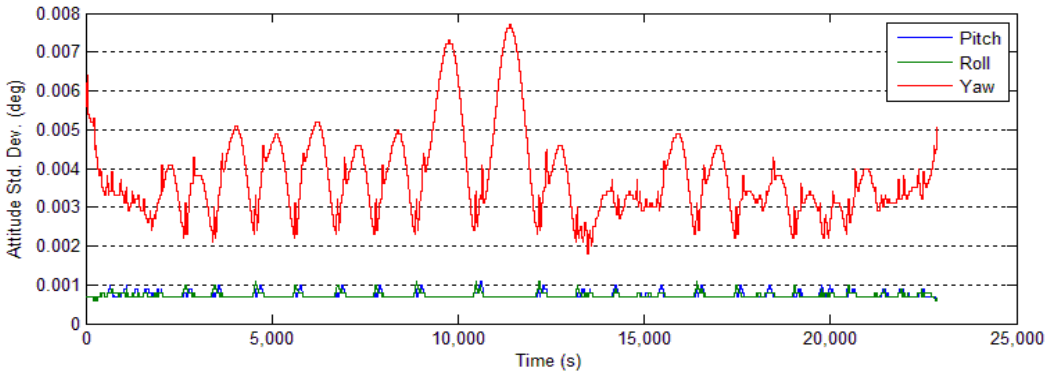

Figure 31. The STD of the attitude angles in the three-direction filtering.

3.4 The Sensor Interface/Acquisition

Precise timing of all the sensory data to GPS time is essential for sensor integration. For more sophisticated use, the GPS time must be externally recovered from the 1PPS signal, available through a standard interface from a GPS receiver. This solution requires timer hardware and control software. The disadvantage of the extra hardware is well offset by the flexibility offered by the excellent time-tagging capabilities of the GPS-synchronized external timing system.

The goal of this task was to develop a conceptual framework and create a design, which was aimed at solving both the timing and the GPS synchronization problem for IMU and other sensors in the assembly. An important aspect of the new design is the limited PC hardware requirement for timing and data recording. While earlier designs usually required a dedicated PC or embedded system for data recording from a single IMU, the new configuration is based on a single PC and can handle synchronization of events from various inputs. Figure 32 shows a typical earlier design, supporting the GPS time tagging of a single IMU. Figure 33 shows the new design, implemented for this project, providing better GPS time tagging capabilities for a multi-sensor system that could include multiple IMUs of various grades (for testing purposes, such as, to facilitate the navigation performance comparison). Obviously, the newer systems have sufficient computer capacity to handle the load of multiple IMU data logging processes, say up to 2-5 IMUs.

The basic concept of this novel design is that the programs, each supporting only one piece of hardware, are running concurrently, and there is no communication between any two programs. A single GPS interface provides a connection to the PC clock and the timing is accomplished by using the high-precision PC clock as a common time base. This solution makes the software developments rather straightforward, as every program deals with only one hardware component. The GPS interface is essential, as without it the GPS synchronization is impossible. However, if the GPS timing is available, there is no real limit with respect to the number of the IMU interface programs, besides the obvious ones, such as the number of available PCI slots and the performance of the PC in terms of sharing the CPU and the storage systems. In the current implementation, there is a hardware timer that provides the link between the GPS and PC times. To GPS time-tag of external events, additional timer boards can be used and, obviously, it is expected to provide much more accurate event timing.

Various sensors can be served by this timing/interface software, as shown in Figures 33-34.

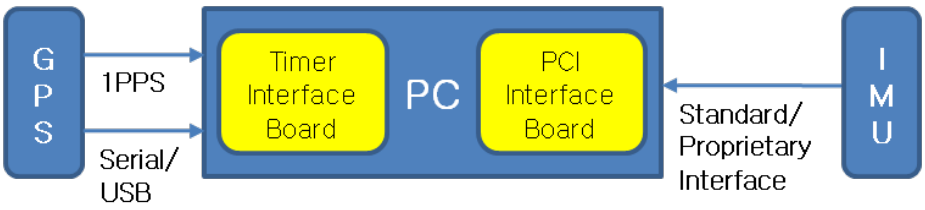

Figure 32. Dedicated single sensor GPS time tagging design.

The PCI-CTR05 timing board used in the current implementation can be programmed either directly via system-level interface, or using a basic driver providing a typical API environment for the user. We chose using the Universal Library from Measurement

Computing, which provides the capability to access the great majority of the function of the AMD9513 timer, yet makes the interface programming simple and system-independent; there is no need to deal with the operating systems changes as the driver is maintained by the manufacturers. The current release of the Universal Library is for Windows 9x/ME/NT 4.0/2000/XP with the language support for C/C++, Delphi, Visual Studio and Visual Studio NET programming languages.

The concept of the software design developed and implemented for this project is shown in Figure 34.

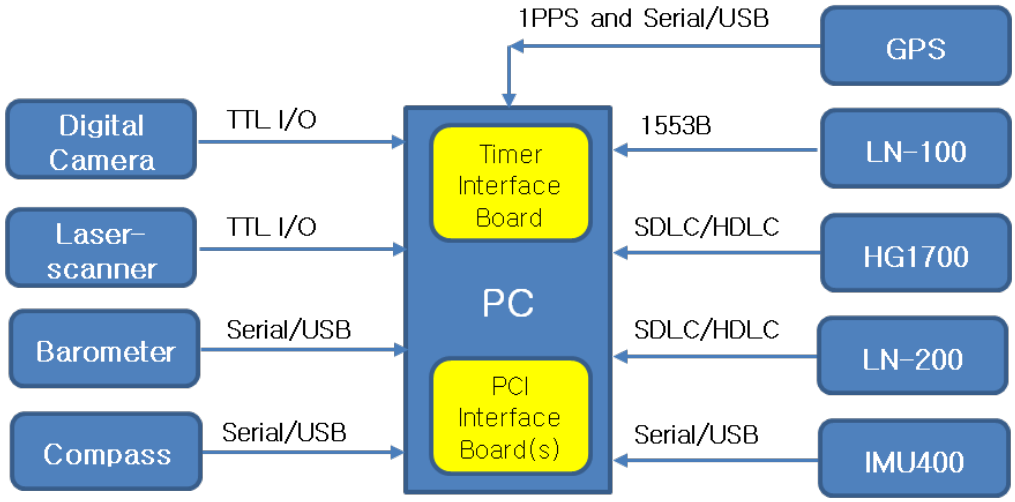

Figure 33. New design to support multi-sensor GPS time tagging.

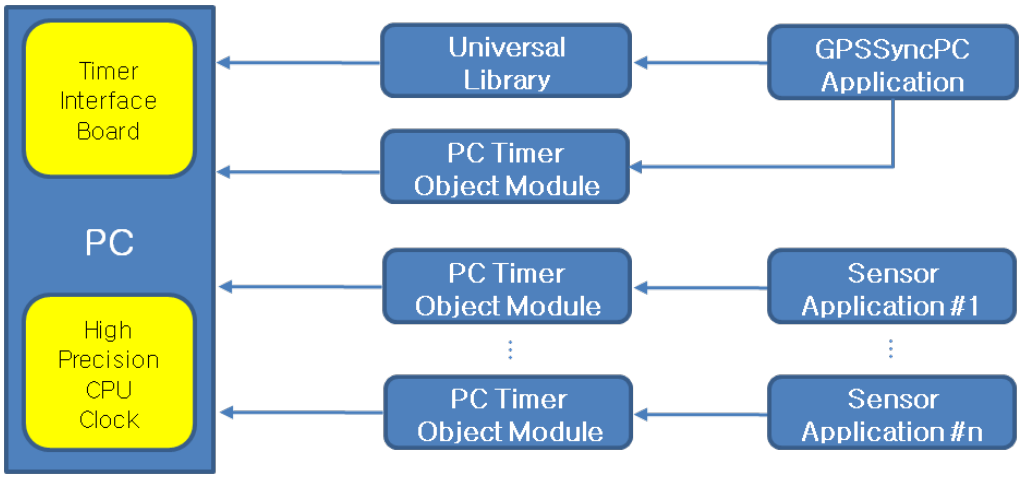

Figure 34. Software design to implement GPS time tagging based the PCI-CTR05 board.

Extensive tests were performed to check the implementation of the transformation between the different time bases, to debug the code, and finally to analyze the performance of the developed GPS time tagging technology. Here, only the final results are presented. A demo dataset was acquired by the prototype system, which had two PCI-CTR05 boards installed. The very same 1PPS signal was used for both purposes to provide: 1) the reference for the GPS timing core, and 2) external event signal for testing. The hardware of the prototype system (shown in Figure 33) was based on a standard Dell desktop PC; 2.66 GHz CPU, 1 GByte RAM, Windows XP with SP2. A Trimble 4000SSI was used as GPS hardware. Four

datasets of various durations were used. There were two objectives of this investigation: 1) to validate the feasibility of the linear model, and 2) to assess the overall accuracy performance.

Concerning the first task, the performance of the hardware timer should be analyzed since it provides the common reference for all the other time bases. The two-board prototype provided an excellent basis for comparisons. Two counter sequences were matched against each other using a simple linear fit. Table 5 summarizes the results in terms of bias and variances estimates. The table clearly shows that for a several-minute period, the linear model is absolutely satisfactory, as the short-term behavior of the hardware is ignorable. In fact, the long-term trend seems rather adequate for many IMUs, where the sampling rate is about 4 ms and the jitter is in the order of tens of μs**.**

Length of the sample [s]	Bias [μs]	STD [μs]
60	0 (5.76E-14)	0.7
300	0 (-2.37E-13)	0.8
1800	0 (-8.91E-13)	2
18000	0 (7.73E-11)	12

Table 5. Performance comparison of two independent hardware counters [64-bit].

Despite the strong evidence for the validity of the linear model, we tested also higher order polynomial models for an 1800 sec dataset, as shown in Table 6.

Polynomial Order	Bias [μs]	STD [μs]
3	0 (9.21E-15)	1.3
2	0 (2.00E-14)	1.4
1	0 (-8.91E-13)	2

Table 6. Comparing higher order polynomial fits.

The ultimate test of the system was when the 1PPS signal was measured by the second board and there was a complete propagation of the time base transformation. Table 7 shows the typical results for the short-term datasets. From the above discussion it is clear that an adaptive linear model represents an adequate approach. The implementation could be a moving average, Kalman filter, etc.

Length of the sample [s]	STD [μs]
60	1
300	1.1
1800	2

Table 7. Performance results of time tagging the external 1PPS signal.

3.5 The multi-senor UXO geolocation system prototype

The prototype of pushcart was assembled and tested in 2009. The pushcart system was equipped with a GPS receiver, a tactical grade IMU (HG1700), and a Trimble GX 3D Laser Scanner (Figure 35). As the PL sensors were not available at the test sites, there was no PL assembled in the pushcart system.

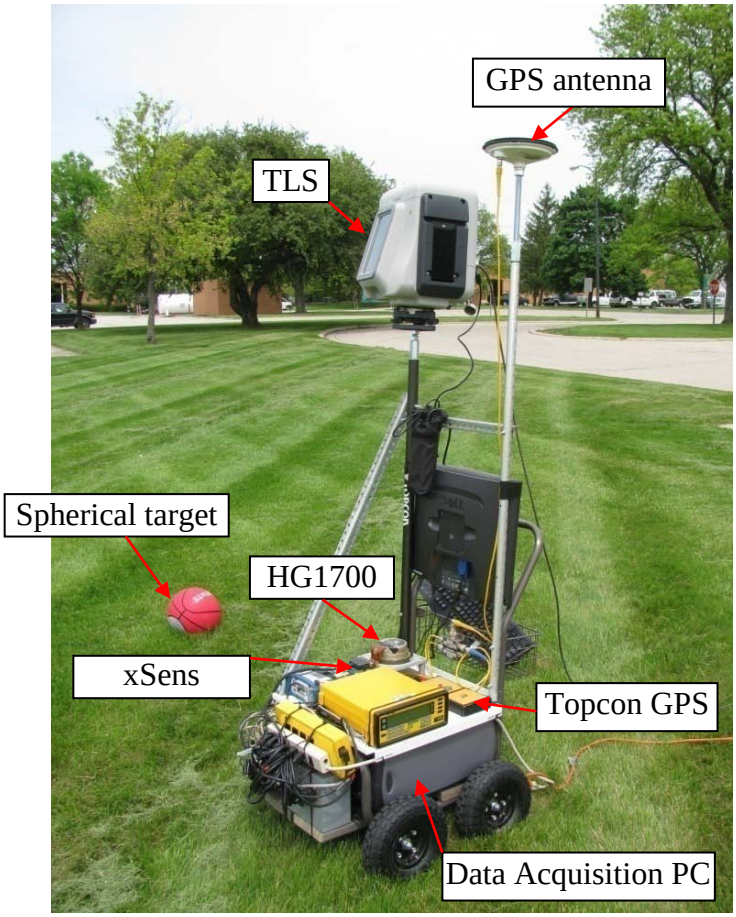

Figure 35. The configuration of the pushcart.

4. Results and Discussion

In cooperation with our partners, the University of New South Wales, there were four field tests carried out in the US and in Australia in 2008. From the 13th to the 18th of March, ten data sets with GPS/Locata/INS were collected in Numeralla, Australia. In this experiments, one Leica 1200 and one Novatel OEM4 GPS receiver (connected to the same antenna) were used as a base station, two Leica 1200 GPS receivers were used as rovers, one OmniStar GPS receiver was used to facilitate time synchronization between GPS and Locata, two dual frequency Locata receivers and an H764G IMU were also used in these experiments. All sensors were assembled on a rigid frame and placed on the top of a truck, as shown in Figure 36. The data sets were used mainly to analyze the integration of GPS/INS/Locata signals and the characteristics of Locata's measurements.

Figure 36. The configuration of the sensors in the test in Numeralla.

The second field campaign took place in June 2008 at OSU. In this test, the complete sensor suite was used, including GPS, INS, Locata and TLS, and five data sets were collected. Unfortunately, the TLS could not be synchronized to other sensors, as the Trimble unit provided by ODOT did not have the hardware interface for GPS timing, and thus, the full integration of GPS/INS/Locata/TLS could not be achieved. The TLS data from this test was only used for the analysis and evaluation of the TLS surface matching algorithms.

The third test took place again in Numeralla, Australia, in July 2008. In this test, a new (in-house developed) GPS time synchronization technique was used for the Locata time tagging. These data were used for further system performance evaluation; there was no TLS data collected in this test.

The forth test at Wright-Patterson Air Force Base in Dayton took place between 10 and 14 of November 2008. In this test, the entire GPS/INS/Locata/TLS sensor suite was time-synchronized; the configuration of the sensors is shown in Figure 37.

Figure 37. The configuration of the sensors in the test at Dayton.

When integrating IMU hardware with other sensors, the sensors should ideally share the very same physical location, which would be optimal from a theoretical point of view. Obviously, it is not possible, and therefore knowing the spatial relationship among the sensors is crucial to achieving the highest possible navigation performance. The displacement vectors or mounting biases are offsets, also called 'lever arms', from the center of the IMU body frame to the centers (reference points) of other sensors. These lever arm parameters may be included in the Kalman filter state vector, as already explained, and thus, they may be estimated for GPS and Locata antenna, as well as for TLS reference point, in the EKF integrated solution. However, in this research, the lever arms were precisely measured during the assembly of the system for GPS and Locata, so only that of TLS needed a calibration. Moreover, since it is impossible to align all TLS axes parallel to those of the IMU, it is also necessary to calculate the boresight misalignment matrix of TLS with respect to the IMU body axes.

An algorithm for the calibration of TLS lever arm offsets and boresight misalignment has been developed. If there are two or more common scanned objects, which can be distinguished with the surface matching results from different sensor locations, the offsets and boresight misalignment can be estimated. The coefficients of the design matrices of the unknown parameters are the differences between the rotation matrices, and the differences between the 3D coordinate offset vectors, respectively. Hence, a significant change in orientation and location of the TLS is required to assure a strong geometry, and thus, to avoid singularity in the calibration solution. Also an iterative estimation method is needed. Our experience indicates that the solution converges in just a few iterations.

The overall system performance for the quadruple sensor integration was further evaluated using the field data collected along an unused runway at the US Air Force Base, in Dayton, Ohio, in November 2008. The sensor configuration, mounted on the top of the GPSVan, included a Novatel OEM4 dual-frequency GPS receiver, a single-frequency Locata receiver, and a Trimble GX3D Laser scanner, as shown in Figure 38; the H764G IMU was mounted inside the vehicle. Ten basketballs were placed on the ground as the spherical targets for laser scanning. The detailed specifications of the sensors are listed in Table 8. The lever arm offsets of the GPS and Locata antennas were measured in the IMU body frame and used as fixed in the AIMS-PRO™ solution. The average separation between the rover and the base GPS was about 1 km, with the number of satellites observed ranging between five and nine, and PDOP between 1.5 and 3.3. There were six LocataLites deployed in the test field, and at least five of them were observed at every epoch of the test. Locata system was synchronized

with the GPS time. The initial ambiguity bias was resolved with data from the GPS carrier phase position.

Since the GPS/INS based navigation solution is well-understood; therefore, the focus was on testing the impact of the Locata signals and on the efficiency of the TLS-based resection. There are three solutions analyzed here: (1) GPS/INS integration with continuous GPS signals, which forms the reference solution; (2) simulated GPS outage scenario in GPS/INS integration, which shows the limits of the INS based navigation; (3) simulated GPS and PL outage scenario in GPS/PL/INS/TLS integration. In cases of (2) and (3), two periods of GPS outages (from P0 to P1 and from P2 to P3), and one period of Locata outage (from P2 to P3) were simulated, as marked in orange in Figure 39. The periods of TLS observations (S0 to S11) are also marked in light green in this figure. The exact times of GPS and PL outages are listed in Table 9.

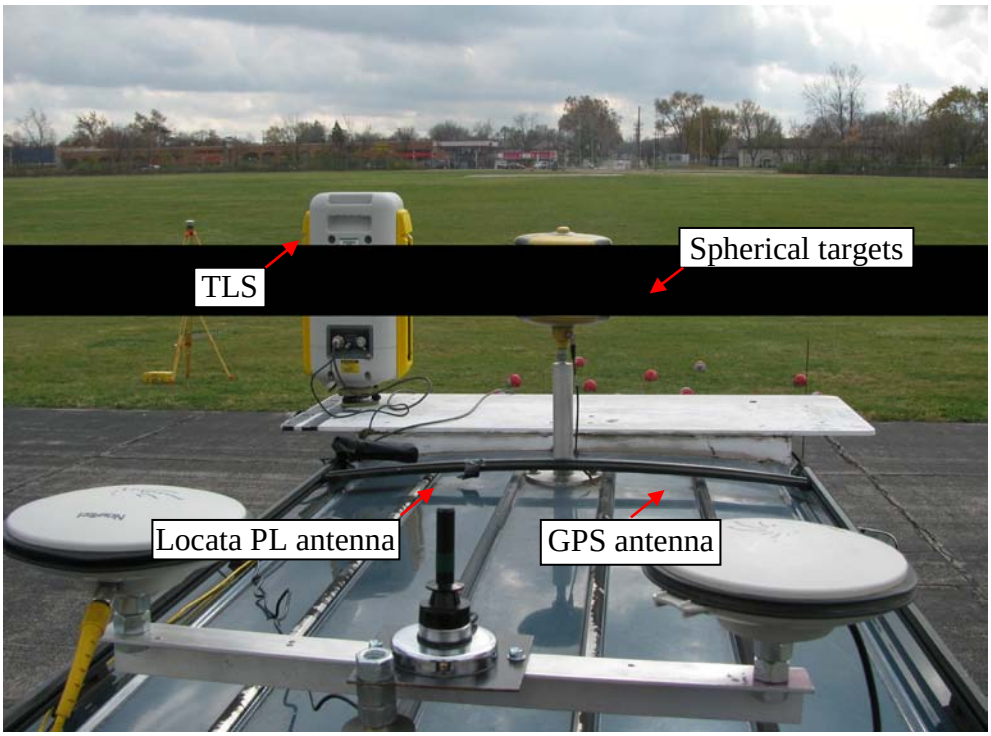

Figure 38. Sensor assembly used in the performance evaluation test in Dayton, OH.

Specifications	IMU		Base GPS	Rover GPS	PL
Model	H764G		Topcon Legacy, dual frequency	OEM4 Dual frequency	Locata Single frequency
Data rate	256Hz		1Hz	10Hz	2Hz
Gyroscope	Bias	0.0035deg/h			
	Scale factor	5 ppm			
	Random walk	0.0035deg/$h^{1/2}$			
Accerolometer	Bias	25μg			
	Scale factor	100 ppm			
	Random walk	0.003 (m/s)/$h^{1/2}$			

Table 8. The specifications of the sensors used in the test (ppm: part per million)

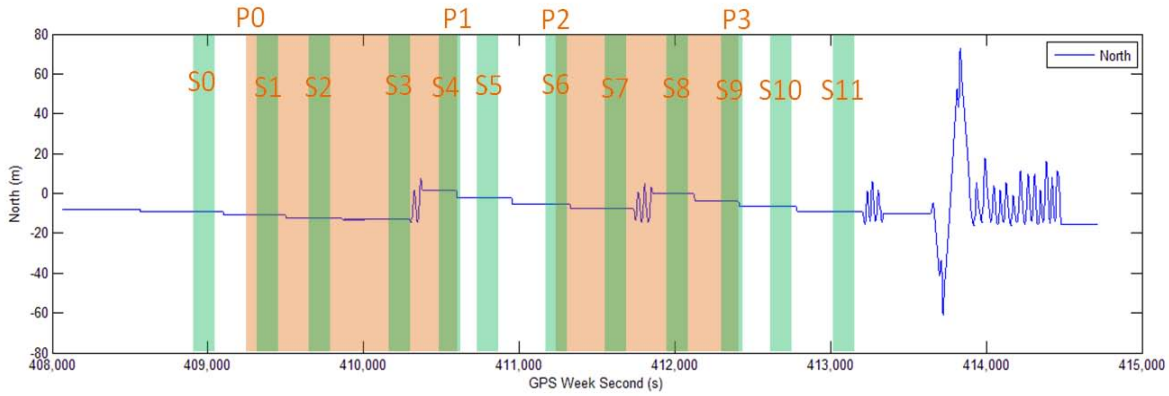

Figure 39. The trajectory in north direction of the vehicle, and simulated blockage of GPS (P0 to P1) and GPS/PL (P2 to P3), and observation periods of static TLS data collection (Time periods marked in green, S0 through S11)

Point	Time (second within the week)	GPS gap (s)	Accumulated GPS gap duration (s)	Accumulated GPS/Locata gap duration (s)
S0	409098.1	0	0	0
P0	409300.0	0	0	0
S1	409499.3	199.3	199.3	0
S2	409859.7	360.4	559.7	0
S3	410297.6	437.9	997.6	0
P1	410500.0	202.4	1200.0	0
S4	410595.5	0	0	0
S5	410950.3	0	0	0
P2	411200.0	0	0	0
S6	411326.9	126.9	126.9	126.9
S7	411733.8	406.9	533.8	533.8
S8	412122.0	388.2	922.0	922.0
P3	412200.0	78.0	1000.0	1000.0
S9	412407.4	0	0	0
S10	412779.6	0	0	0
S11	413205.6	0	0	0

Table 9. The test points and the corresponding simulated GPS gaps along the test trajectory for Locata and TLS-based IMU calibration.

4.1 GPS/INS integration

In the GPS/INS integration scenario, only double difference GPS carrier phase observations were used as EKF measurement updates. Figures 40-43 illustrate the standard deviation (STD) of the coordinates and attitude together with the corresponding coordinate and attitude errors estimated by EKF. It can be observed in Figures 40 and 41 that the position errors were at the level of a few centimeters with a cm-level STD. As shown in Figure 42, the STD of pitch and roll was ~0.002°, and the STD of heading was between 0.05° and 0.15°, primarily due to the limited maneuvering of the vehicle. By the end of the test, the heading became resolved with a STD of ~0.02°.

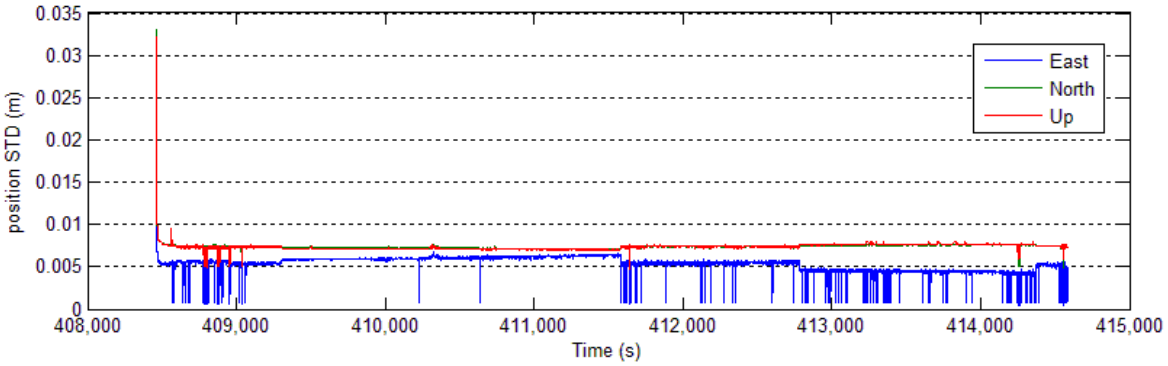

Figure 40. The standard deviation of the estimated coordinates in the GPS/INS solution.

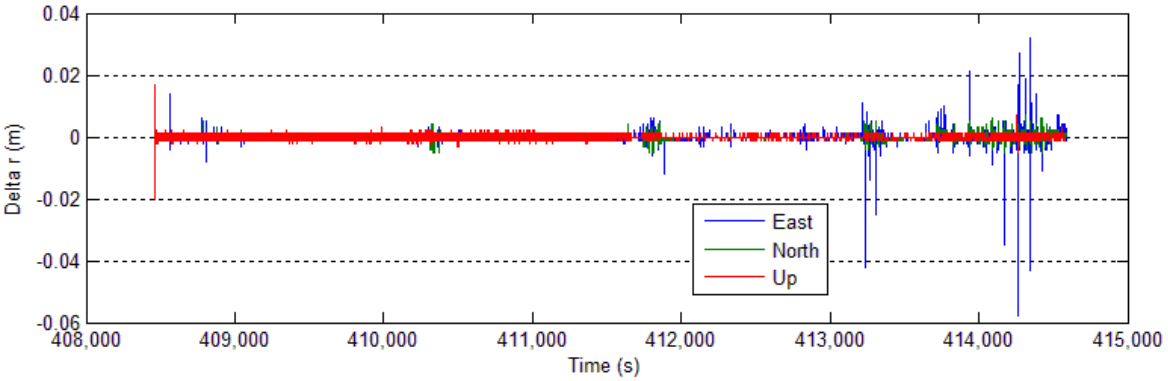

Figure 41. The EKF position error sub-state in the GPS/INS solution.

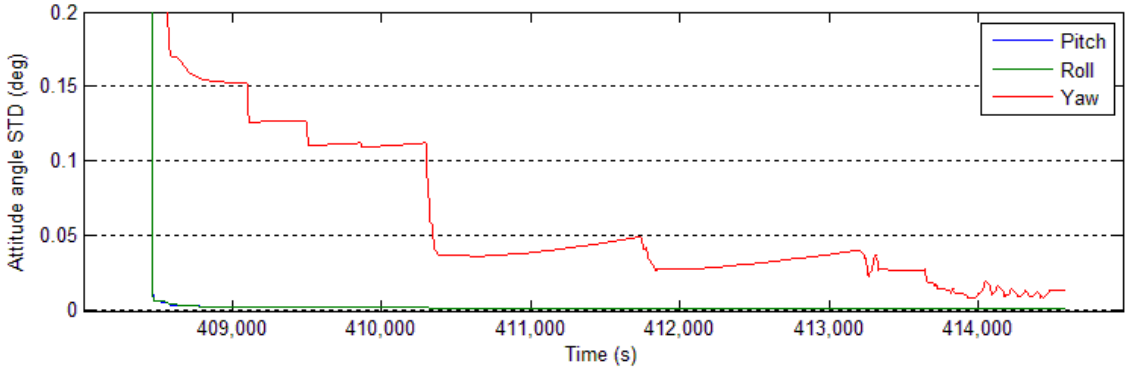

Figure 42. The standard deviation of the estimated attitude angles in the GPS/INS solution.

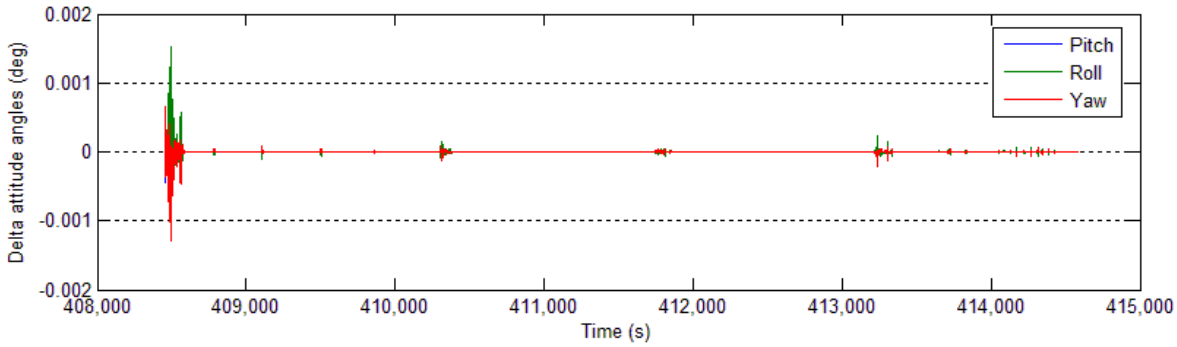

Figure 43. The EKF attitude angle error sub-state in the GPS/INS solution.

4.2 GPS/INS integration with simulated GPS outages

In the GPS/INS solution with simulated GPS outages, as marked in Figure 39, the 3D navigation errors of the H764G IMU during the two GPS outages were around 144 m and 231 m, respectively (see Table 10 for details). Figure 44 depicts the trajectory of the stand alone inertial navigation during a simulated GPS outage, and the reference GPS/INS solution. The two straight segments of the INS-only trajectory correspond to ~10-minute vehicle stops, where the IMU solution drifted significantly.

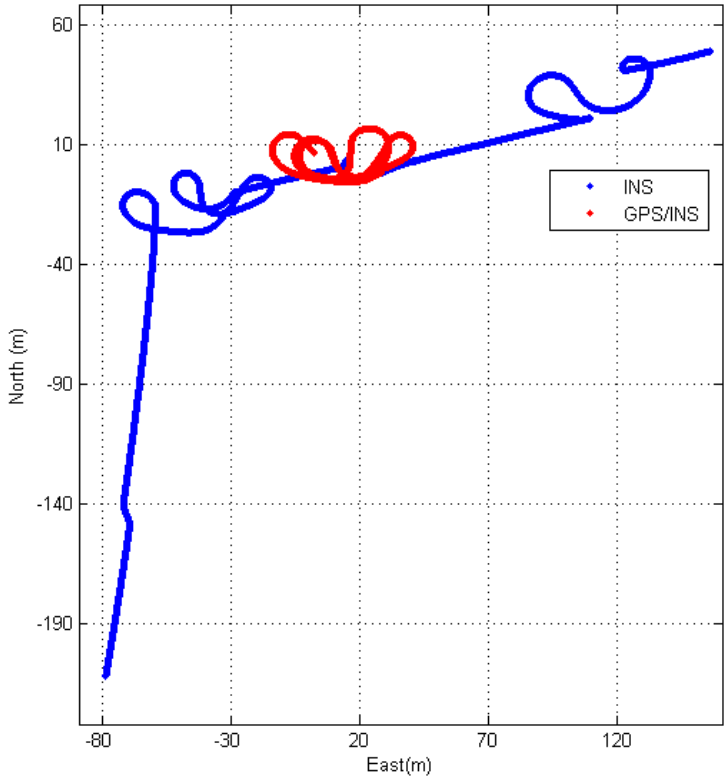

Figure 44. The trajectory of standalone IMU navigation period during GPS outage and the corresponding GPS/INS trajectory.

Site	Scenario	East (m)	North (m)	Height (m)	ΔE (m)	ΔN (m)	ΔH (m)	3D Error
S1	1	499988.3460	4404395.7307	207.5574				
	2	499989.6635	4404396.4987	207.8835	1.318	0.768	0.326	1.560
	3	499988.3472	4404395.7284	207.5580	0.001	-0.002	0.001	0.002
S2	1	499985.0889	4404393.9753	207.5526				
	2	500001.8085	4404400.9303	210.1586	16.720	6.955	2.606	18.295
	3	499985.0913	4404393.9705	207.5536	0.002	-0.005	0.001	0.006
S3	1	499983.6912	4404393.2238	207.5295				
	2	500068.5720	4404418.3771	219.3914	84.881	25.153	11.862	89.321
	3	499983.6944	4404393.2179	207.5301	0.003	-0.006	0.001	0.007
P1	1	499976.8965	4404408.3793	207.6011				
	2	500115.0023	4404446.1118	228.0126	138.106	37.732	20.412	144.615
	3	499976. 9008	4404408.3726	207.6030	0.004	-0.007	0.002	0.008
S6	1	499976.3145	4404401.4269	207.5435				
	2	499974.8632	4404400.9243	207.5629	-1.451	-0.503	0.019	1.536
	3	499976.3086	4404401.4124	207.5439	-0.006	-0.014	0.001	0.015
S7	1	499976.1537	4404399.2014	207.5170				
	2	499931.7609	4404387.4376	207.0399	-44.393	-11.764	-0.477	45.928
	3	499976.1497	4404399.1868	207.5182	-0.004	-0.015	0.001	0.016
S8	1	499959.2946	4404407.5353	207.4743				
	2	499889.0641	4404258.2254	204.2422	-70.230	-149.310	-3.232	165.034
	3	499959.2823	4404407.5051	207.4729	-0.012	-0.030	-0.001	0.032
P3	1	499962.4777	4404403.9876	207.4753				
	2	499882.2938	4404186.5778	203.0632	-80.184	-217.410	-4.412	231.767
	3	499960.9027	4404403.1491	207.1254	-1.575	-0.838	-0.350	1.818

(Note: Scenario 1 denotes GPS/INS integration; Scenario 2 denotes GPS/INS integration with simulated GPS outage; Scenario 3 denotes GPS/Locata/INS/TLS integration with simulated GPS/Locata outage)

Table 10. Estimated TLS coordinates in the three tested scenarios and the differences between scenarios 2 and 3 with respect to scenario 1 (reference trajectory) for GPS/INS/PL/TLS integration.

4.3 GPS/PL/INS/TLS integration with simulated GPS and PL outages

During the simulated GPS blockage with Locata signals available, Locata was able to maintain high accuracy navigation solution, as illustrated in Figure 45. During the simultaneous blockages of both GPS and Locata signals, the navigation accuracy is based on the stand-alone IMU. However, if TLS data are available at static locations, the IMU error calibration is possible at that locations and centimeter-level navigation accuracy is achievable.

The test results indicate that the Locata system is able to calibrate the IMU errors with the level of accuracy comparable to GPS. Figure 45 shows the coordinate STD at every measurement update during the first GPS blockage, which was mainly calibrated by the PL signal, periodically supported by the TLS-based resection (see Figure 39 for exact time periods when TLS was operational during the GPS and PL gaps). A comparison of scenarios 1 (reference GPS/INS solution) and 3 (INS supported by PL/TLS) at point P1 shows

coordinate differences of 0.004m, -0.007m and 0.002m, respectively, proving that PL is indeed capable of maintaining cm-level navigation accuracy during GPS signal outage (Table 10).

By inspecting the results at point P3, listed in Table 10, it is clear that the TLS limits the IMU errors, reducing the 3D absolute navigation error from about 231.7 m (scenario 2) to max 1.8 m (scenario 3) with respect to the reference trajectory (scenario 1). Notice that the 1.8 m absolute error results predominantly from the fact that the system was navigating in a free-inertial mode for 78 seconds between points S8 and P3 (refer to Figure 39 for a list of simulated signal outages and TLS observation periods). The coordinate differences between the TLS-supported navigation solutions (scenario 3) with respect to the reference trajectory (scenario 1) at points S1 through S8 are at the cm-level. This clearly indicates that TLS can calibrate the IMU errors, while the free-inertial navigation solution (scenario 2) at these points is subject to errors ranging from few centimeters to more than a hundred meters per coordinate.

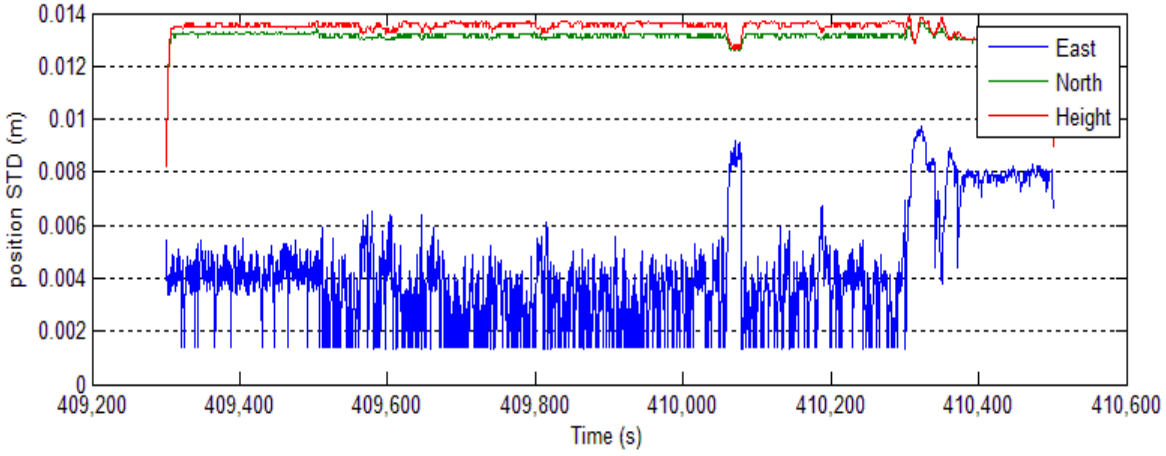

Figure 45. The position standard deviation of the Locata/INS integration during the period of first GPS blockage.

It is necessary to point out that the high absolute accuracy during the second GPS/Locata blockage (P2 to P3) was due to GPS/Locata observations collected at the previous scanning sites, S0-S5. If there were no GPS/Locata observations at these scanning sites, the absolute position error of the system would have been impacted by the drifting IMU sensors.

4.4 Calibration of TLS lever arm offsets and boresight misalignment

As mentioned earlier, the lever arm offsets and boresight misalignment angles of the TLS reference frame with respect to the IMU body axes can be calibrated using a reference GPS/INS solution. In order to test our calibration algorithm, the TLS-IMU lever arm offsets were measured with a centimeter-level accuracy before the calibration as (-0.596m, 1.559m, 1.036m) for right, front and up directions, respectively. The solution of scenario 1 (GPS/INS integration) and all observations at all TLS scanning sites were used for the calibration that was performed as the least squares adjustment. The calibration results are shown in Table 11, and the observation residuals are plotted in Figure 46.

Contents	Lever arm (m)			Misalignment angles (deg)		
	Right	Front	Up	Pitch	Roll	Yaw
Value	-0.592	1.592	-2.481	0.005	-0.004	28.961
(ref)	-0.596	1.559	1.036	n/a	n/a	n/a
(dif)	0.008	-0.033	-3.517	n/a	n/a	n/a
Std. Dev.	0.003	0.001	0.174	0.006	0.019	0.007

Table 11. The lever arm offsets and boresight misalignment angles of TLS obtained by the calibration procedure.

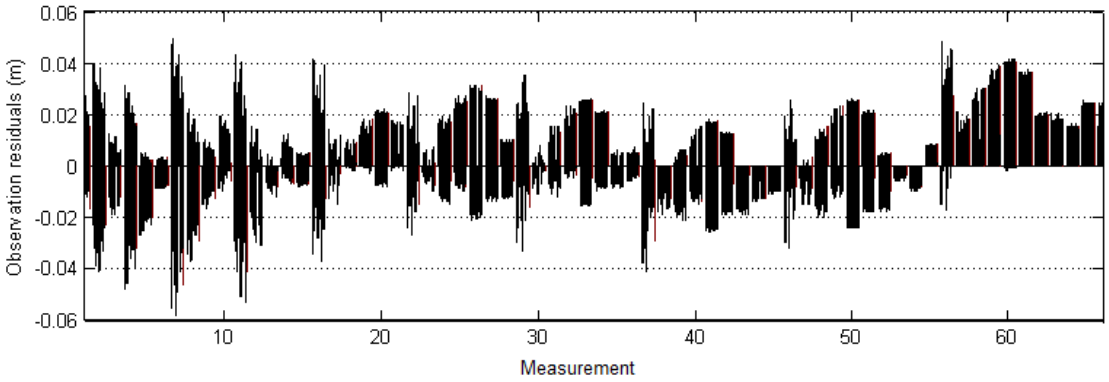

Figure 46. Observation residuals from the least squares estimation of the lever arm offsets and boresight angles.

In Figure 46, the coordinate residuals of the scanned targets used in the calibration procedure are generally no bigger than 4 cm. It can be observed in Table 11 that the standard deviations of boresight misalignment angles are 0.006° for pitch, 0.007° for yaw, and 0.02° for roll. The standard deviation of the lever arm offsets is at a few-millimeter level for the right and the front, and a few decimeters for the up component. The poor accuracy for the roll misalignment and the vertical lever arm is due to the weak geometry in the calibration configuration. During the tests, all the spheres were put on flat grounds and the vehicle did not experience significant changes in pitch or roll, which resulted in the limited vertical change in the coordinates of the spherical targets. Also, the vehicle faced the spheres during the scanning process, so the lateral distance from the spheres to the vehicle was limited, which translated to a weak detection of the change in vehicle's roll. The comparison of the lever arm offset calibration results shown in Table 11 with the measured values, reveals a difference of 0.008m, -0.033m and -3.517m in three components, respectively. This verifies the calibration efficiency for the horizontal components of the lever arm offsets, but confirms the inability to resolve the vertical component. In the processing of GPS/PL/INS/TLS integration, the measured vertical lever arm offset (1.036 m) was used.

4.5 Estimation of the coordinates of spherical target centers from TLS point cloud and target matching

In tests at the US Air Force Base, in Dayton, Ohio, in November 2008, TLS data were collected at 12 sites with ten spherical targets used as matching objects. The spherical target coordinate estimation and matching were accomplished using the earlier developed algorithms. The results of the target center coordinate estimation for site S0 are given in Table 12 as an example. The accuracy of the estimated target centers is generally better than 2 millimeters, and the algorithm converged in 2 to 3 iterations, even when only ~110 points on the target were available; note that these ideal conditions may not be realistic in less prevalent environments, though it should be well within the requirements. The point cloud of an example target is shown in Figure 47. The average difference in distances between any two given targets observed from the first and last scanning sites, as shown in see Figure 48, is 1.9 mm with the corresponding standard deviation of 4.1 mm.

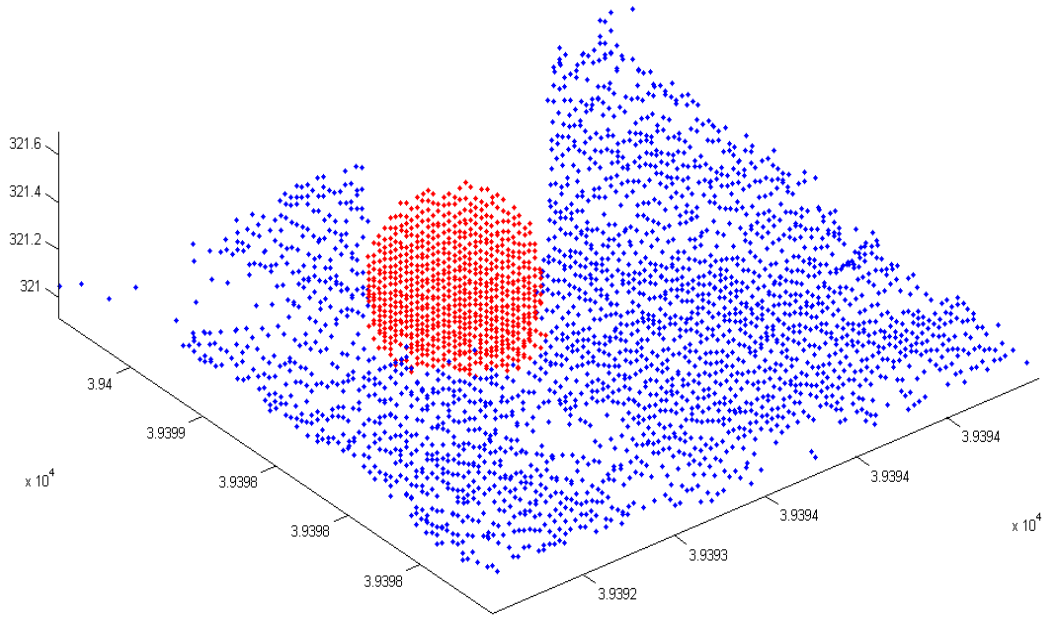

Figure 47. The extracted points of target 1 (red) and the neighboring points (blue). Units: (m).

Sphere	X (m)	Y (m)	Z (m)	Std. Dev. (m)	Points	Iteration
1	1.916	14.876	-2.135	0.0011	266	2
2	0.168	16.258	-2.216	0.0010	255	3
3	3.155	16.306	-2.170	0.0009	249	2
4	1.529	16.950	-2.202	0.0013	189	2
5	1.215	18.679	-2.205	0.0014	182	2
6	3.094	17.795	-2.216	0.0014	160	3
7	0.895	18.846	-2.246	0.0014	157	2
8	4.688	19.209	-2.212	0.0015	136	3
9	2.773	20.910	-2.281	0.0018	113	2
10	0.438	20.502	-2.266	0.0019	112	3

Table 12. The coordinates of the estimated centers of the spherical targets in the TLS data set collected at site S0.

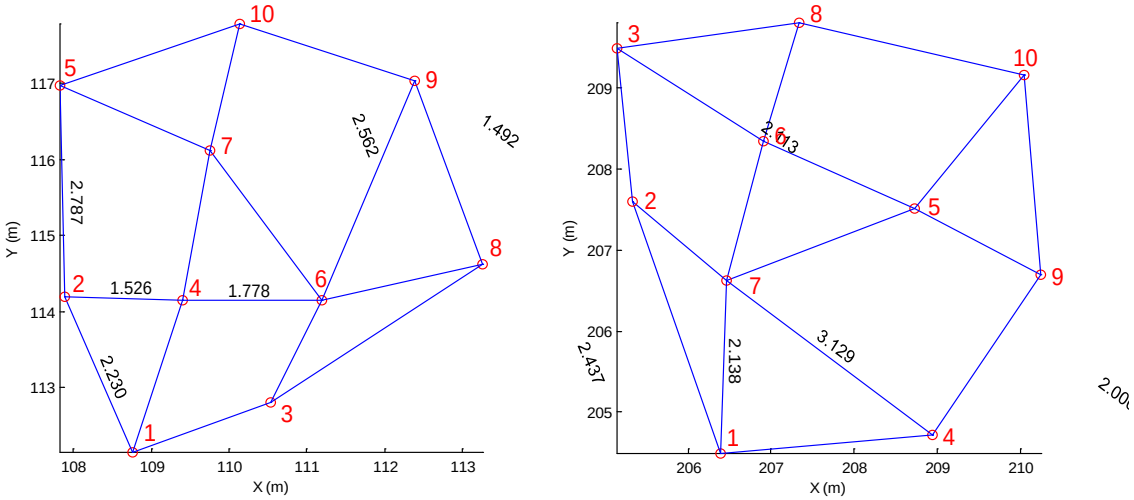

Figure 48. Estimated locations and the corresponding connecting distances (m) of the spherical target centers of the first and the last TLS scans, shown in TLS frames.

5. Conclusions and Implications for Future Research/Implementation

The MEC characterization and remediation activities using currently available technology (mostly, RTK-GPS) often yields unsatisfactory results due mainly to the inability of current navigation technology to provide the precise position and orientation information. This results in poor geolocation of the acquired electromagnetic imagery and consequently, the inability to discriminate between MEC and non-hazardous items in the imagery. Reliable and precise geolocation technology is essential for robust detection and discrimination of unexploded ordnance (UXO) in various field conditions.

The main achievement of this research is the integration of PL and GPS signals together with INS and TLS measurements in the form of quadruple GPS/INS/PL/TLS integration system, which can deliver high accuracy multi-sensor positioning solution and is compatible with magnetic and electromagnetic geophysical sensors. Second, for the optimal data processing the new software, named as AIMS-PRO™, was designed and implemented to incorporate the concept of a novel quadruple integration of GPS (GNSS), PL, INS, and TLS. Third, precise timing of all the sensory data to GPS time was designed and efficiently implemented. Finally, a demonstration prototype was designed, implemented and tested. The navigation technologies developed under this research will allow accurate and reliable operations of new and emerging UXO detection sensors, where precise sensor location and orientation are required.

The overall system performance of the quadruple GPS/INS/PL/TLS integration system was evaluated using the real field data collected mainly in 2008. Test results have demonstrated the ability of the system to maintain the required accuracy level (cm-accurate positioning) in difficult environments where long GPS outages (in the range from 200 to 900 seconds) can be anticipated. Improved performance of the UXO geolocation system will aid significantly in the inversion of field data for more accurate characterization of candidates for buried

munitions, thus greatly reducing the number of false positives, which currently can reach 90% or more. The milestones of the project developments and relevant publications are listed in Table 13.

To further improve the current algorithmic solution, it is proposed for the Phase 2 of this project to incorporate deeply integrated GPS signal processing into the quadruple navigation solution in order to enhance the navigation robustness and, optionally, to relax the system operational requirements. That is expected to lower the complexity of its installation and maintenance, as well as the overall cost, size, weight and power consumption. This will be achieved by extending the multi-sensor fusion that is currently performed at the sensor measurement level into the signal processing level. The proposed modification will enable GPS measurements under severe signal attenuation (such as a 30 dB or a factor of 1000 power attenuation from open sky conditions). Augmenting the system with the capability to maintain GPS measurements for very weak signals will increase significantly the GPS coverage in difficult environments, such as under dense canopy. Increased availability of GPS measurements will improve the robustness of the navigation solution. Specifically, additional GPS measurements can be efficiently exploited for the identification of GPS and PL signals that are corrupted by multipath reflections from surrounding trees. The increased GPS availability will enable reduction of the system operational requirements. Particularly, it is expected that the incorporation of deep integration will decrease the need for the pseudolite-based navigation, and thus, will potentially minimize the deployment complexity of the TLS component, as well as reduce the requirements to inertial sensor performance.

Year	Date	Location	Collaborators	Sensors	Platform	Objective/Method	Performance Evaluation	Achieved Performance
2007							Assessment report on expected performance	n/a
2008	March	Numarella, Australia	UNSW, Locata	GPS/IMU/PL	Test vehicle	PL sensor characterization and performance assessment	Performance testing of GPS/IMU system, initial testing of PL performance in simulated environment	n/a
	June	OSU Campus	UNSW, ODOT	GPS/IMU/PL/TLS	Test vehicle (GPSVan)	PL and TLS sensor characterization and performance assessment	Initial testing of TLS performance in simulated and real environment	<1 cm (TLS-only)
	July	Numarella, Australia	UNSW, Locata	GPS/IMU/PL	Test vehicle	PL timing investigation, characterization and performance assessment	Performance testing of PL system, initial testing of overall performance in simulated and real environment	2-5 cm (GPS/IMU) 3-15 cm (PL/IMU)
	August	Dayton, OH	AFRL	GPS/IMU	Test vehicle (GPSVan)	GPS/IMU integration validation	Field testing GPS/IMU performance	1-2 cm (GPS/IMU)
	November	Dayton, OH	AFRL/AFIT, ODOT	GPS/IMU/PL/TLS	Test vehicle (GPSVan)	GPS/IMU/PL/TLS integration validation	Field testing GPS/IMU/PL/TLS performance	1-2 cm (GPS/IMU/PL/TLS)
2009	May	Columbus, OH	ODOT	GPS/IMU/TLS	Pushcart prototype	GPS/IMU/TLS integration validation	Field testing GPS/IMU/TLS performance	1-2 cm (GPS/IMU/TLS)
	August	OSU Campus		GPS/IMU	Pushcart prototype	GPS/IMU pushcart system testing	Testing related to system design recommendation	1-2 cm (GPS/IMU)
2010							Final report preparation	n/a

Table 13. Project developments and accomplishments, measured in performance evaluation tests.

Publications reporting the project achievements:

1. Grejner-Brzezinska, D.A., C. K. Toth, H. Sun, X. Wang, and C. Rizos (2010): A Robust Solution to High-Accuracy Geolocation: Quadruple Integration of GPS, IMU, Pseudolite and Terrestrial Laser Scanning, *IEEE Transactions on Instrumentation and Measurement*, in print.
2. Chris Rizos, C., D. A. Grejner-Brzezinska, C. K. Toth, A. G. Dempster, Y. Li, N. Politi, J. Barnes, H. Sun, and L. Li (2010): Hybrid Positioning: A Prototype System for Navigation in GPS-Challenged Environments, *GPS World*, Innovation Column, March pp. 42-47.
3. Toth, C. K., Grejner-Brzezinska, D.A., J. Oh, J. N. Markiel (2009): Terrain–based navigation: a tool to improve navigation and feature extraction performance of mobile mapping systems, *Boletim de Ciências Geodésicas*, v. 15, n. 5 pp. 807-823.
4. Wang, X., D. A. Grejner-Brzezinska, C. K. Toth and J-K. Lee (2010): Sensitivity Analysis of Object Space Geometry for TLS-Aided Navigation, Proceedings, ION/IEEE PLANS Palm Springs, May 4-6, CD ROM, pp. 850-857.
5. Wang, H., C. Toth, D. Brzezinska and H. Sun (2008), Integration of Terrestrial Laser Scanner for Ground Navigation in GPS-Challenged Environments, *International Archives of Photogrammetry and Remote Sensing*, Vol. XXXVII, Part B5, pp. 513-519.
6. Rizos C., D. A. Grejner-Brzezinska, C. K. Toth, A. G. Dempster, Y. Li, N. Politi, J. Barnes, H. Sun (2008): A hybrid system for navigation in GPS-challenged environments: case study, Proceedings, ION GNSS, Savannah, Georgia, Sept. 16-19, CD ROM.
7. Toth, C.K., Grejner-Brzezinska, D. A., Shin, S-W., Kwon, J. (2008). A Method for Accurate Time Synchronization of Mobile Mapping Systems, *Journal of Applied Geodesy*, Vol. 2, pp. 159-166.
8. Grejner-Brzezinska, D. A., C. Toth, H. Sun, X. Wang and C. Rizos (2008): GPS/INS/PL/TLS Integration Supporting Navigation of Geophysical Sensors for Unexploded Ordnance Detection And Discrimination, Proceedings, 13th FIG International Symposium on Deformation Measurements and Analysis 4th IAG Symposium on Geodesy for Geotechnical and Structural Engineering, Lisbon, May 12-15 2008, CD ROM.
9. Grejner-Brzezinska, D. A., C. Toth, H. Sun, X. Wang (2008): Novel geolocation technology for geophysical sensors for detection and discrimination of unexploded ordnance, Proceedings, IEEE/ION PLANS Meeting, May 5-8, 2008, Monterey, California, CD ROM.

References

1. Barnes, J., Rizos, C., Wang, J., Small, D., Voigt, G., Gambale, N. (2003a): Locata: A new positioning technology for high precision indoor and outdoor positioning, 16th Int. Tech. Meeting of the Sat Div of the U.S. Inst. of Navigation, Portland, Oregon, 9-12 September.
2. Barnes, J., Rizos, C., Wang, J., Small, D., Voigt, G., Gambale, N. (2003b): High precision indoor and outdoor positioning using LocataNet, 2003 Int. Symp. on GPS/GNSS, Tokyo, Japan, 15-18 November, 9-18.
3. Barnes, J., Rizos, C., Kanli, M., Pahwa, A., Small, D., Voigt, G., Gambale, N., & Lamance, J., (2005): High accuracy positioning using Locata's next generation technology, 18th Int. Tech. Meeting of the Sat Div of the U.S. Institute of Navigation, Long Beach, California, 13-16 Sept, 2049-2056.
4. Cabler, H. (2002): GPS Modernization, A path toward improved capabilities, CAR/SAM ATN/GNSS Seminar, Varadero, Cuba, May 2002.
5. Grejner-Brzezinska, D.A., Kashani, I., and Wielgosz, P. (2005a): On Accuracy and Reliability of Instantaneous Network RTK as a Function of Network Geometry, Station Separation, and Data Processing Strategy, *GPS Solutions,* Vol. 9, No. 3, pp. 179 – 193.
6. Grejner-Brzezinska, D. A., Toth, C. K., Sun, H., Wang, X., and Rizos C., (2010). A robust solution to high-accuracy geolocation: quadruple integration of GPS, IMU, pseudolite and terrestrial laser scanning", IEEE Transactions on Instrumentation and Measurement, in print.
7. Grejner-Brzezinska, D. A., C. Toth, H. Sun, X. Wang and C. Rizos (2008a): GPS/INS/PL/TLS Integration Supporting Navigation of Geophysical Sensors for Unexploded Ordnance Detection And Discrimination, Proceedings, 13th FIG International Symposium on Deformation Measurements and Analysis 4th IAG Symposium on Geodesy for Geotechnical and Structural Engineering, Lisbon, May 12-15 2008, CD ROM.
8. Grejner-Brzezinska, D. A., C. Toth, H. Sun, X. Wang (2008b): Novel geolocation technology for geophysical sensors for detection and discrimination of unexploded ordnance, Proceedings, IEEE/ION PLANS Meeting, May 5-8, 2008, Monterey, California, CD ROM.
9. Gruen, A. and Akca, D. (2005): Least Squares 3D Surface Matching, Proceedings of ASPRS 2005 Annual Conference, Baltimore, Maryland March 7-11.
10. Kashani, I., Grejner-Brzezinska, D.A., and Wielgosz, P., (2005): Towards Instantaneous Network-Based RTK GPS Over 100 km Distance, submitted to Navigation.
11. Li, L., Pan, Y., Grejner-Brzezinska, D.A., Toth, C.K., Sun, H., (2010): Allan Variance Analysis of the H764G Stochastic Sensor Model and its Application in Land Vehicle Navigation, Proceedings of the 2010 International Technical Meeting of The Institute of Navigation, January 25 - 27, 2010, Catamaran Resort Hotel, San Diego, CA.
12. Ogundana, O., Coggrave, C., Burguete, R., and J. Huntley (2007). Fast Hough transform for automated detection of spheres in three-dimensional point clouds. Optical Engineering 46 (5) 051002.

13. Politi N., Yong L. ,Faisal K., Mazher C., Bertsch J.,Cheong J,. Dempster A., Rizos C., (2009) Locata: A New Technology for High Precision Positioning.

14. Rizos C., C., D. A. Grejner-Brzezinska, C. K. Toth, A. G. Dempster, Y. Li, N. Politi, J. Barnes, H. Sun, and L. Li (2010): Hybrid Positioning: A Prototype System for Navigation in GPS-Challenged Environments, *GPS World*, Innovation Column, March pp. 42-47.

15. Rizos C., D. A. Grejner-Brzezinska, C. K. Toth, A. G. Dempster, Y. Li, N. Politi, J. Barnes, H. Sun (2008): A hybrid system for navigation in GPS-challenged environments: case study, Proceedings, ION GNSS, Savannah, Georgia, Sept. 16-19, CD ROM.

16. Vollath, U., Buecherl, A., Landau, H., Pagels, C., and Wagner, B., (2000): Multi-Base RTK ositioning Using Virtual Reference Stations, ION GPS, 19–22 September 2000, Salt Lake City, UT, pp. 123–131.

17. Wanninger, L. (2002): Virtual Reference Stations for Centimeter-Level Kinematic Positioning. ION GPS 2002, September 24–27, Portland, Oregon, pp. 1400–1407.

18. Wang, X., Grejner-Brzezinska, D.A., Toth, C.K., Lee, J-K., 2010. Sensitivity analysis of object space geometry for TLS-aided navigation", Proceedings of the 2010 IEEE/ION Position, Location and Navigation Symposium, Indian Wells/Palm Springs, CA, May 2010, pp. 850-857.